AWARD NUMBER: W81XWH-13-1-0449

TITLE: Differential Splicing of Oncogenes and Tumor Suppressor Genes in African- and Caucasian-American Populations: Contributing Factor in Prostate Cancer Disparities?

PRINCIPAL INVESTIGATOR: Norman H Lee, PhD

CONTRACTING ORGANIZATION: George Washington University School of Medicine
Washington, DC 20052

REPORT DATE: October 2016

TYPE OF REPORT: Annual

PREPARED FOR: U.S. Army Medical Research and Materiel Command
Fort Detrick, Maryland 21702-5012

REPORT DOCUMENTATION PAGE

Form Approved
OMB No. 0704-0188

1. REPORT DATE	2. REPORT TYPE	3. DATES COVERED
October 2016	Annual	30Sep2015 - 29Sep2016

4. TITLE AND SUBTITLE

Differential Splicing of Oncogenes and Tumor Suppressor Genes in African- and Caucasian-American Populations: Contributing Factor in Prostate Cancer Disparities?

5a. CONTRACT NUMBER
W81XWH-13-1-0449

5b. GRANT NUMBER
PC121975

5c. PROGRAM ELEMENT NUMBER

6. AUTHOR(S)

Norman H Lee, PhD; Bi-Dar Wang, PhD; Jacqueline Olender (PhD graduate student)

E-Mail: nhlee@gwu. edu

5d. PROJECT NUMBER

5e. TASK NUMBER

5f. WORK UNIT NUMBER

7. PERFORMING ORGANIZATION NAME(S) AND ADDRESS(ES)

George Washington University School of Medicine
2300 I Street, NW
Ross Hall
Washington, DC 20037

8. PERFORMING ORGANIZATION REPORT NUMBER

9. SPONSORING / MONITORING AGENCY NAME(S) AND ADDRESS(ES)

U.S. Army Medical Research and Materiel Command
Fort Detrick, Maryland 21702-5012

10. SPONSOR/MONITOR'S ACRONYM(S)

11. SPONSOR/MONITOR'S REPORT NUMBER(S)

12. DISTRIBUTION / AVAILABILITY STATEMENT

Approved for Public Release; Distribution Unlimited

13. SUPPLEMENTARY NOTES

14. ABSTRACT

The overarching goal of this grant award is to characterize differential splicing of oncongenes and tumor suppressor genes in prostate cancer disparities between African American (AA) and Caucasian American (CA) prostate cancer (PCa). In years 1-2, we described the molecular cloning of a novel phosphatidylinositol-4,5-bisphosphate 3-kinase 110 kDa catalytic subunit (*PIK3CD*) mRNA variant that is uniquely expressed in AA PCa specimens. This AA-enriched variant is referred to as the short variant of *PIK3CD* (*PIK3CD-S*), which is missing exon 20 due to an exon skipping event. We demonstrated that the *PIK3CD-S* variant: i) encodes a more aggressive oncogenic signaling protein as defined by *in vitro* assays and mouse xenograft studies, ii) is associated with worse prognosis in patients, and iii) is resistant to small molecule inhibitor idelalisib or CAL-101 (selective PI3KCδ inhibitor; FDA approved for treating hematologic cancers). Our discovery portends a genetic screening test for patients with aggressive tumors that are resistant to idelalisib therapy. In year 3 of this award, we have focused our efforts on characterizing the molecular mechanism underlying increased oncogenic signaling by PI3KCδ-S compared to PI3KCδ-L (expressed in CA PCa). Our findings demonstrate that PI3KCδ-L preferentially complexed with the regulatory subunit p85α, leading to decreased kinase activity compared to PI3KCδ-S that has lower affinity for p85α. PI3KCδ-L, in the absence of p85α, exhibited kinase activity comparable to PI3KCδ-S but was still sensitive to the inhibitory effects of idelalisib.

15. SUBJECT TERMS

prostate cancer, cancer health disparities, alternative splicing, African American, European American, oncogenes, tumor suppressor genes

16. SECURITY CLASSIFICATION OF:			17. LIMITATION OF ABSTRACT	18. NUMBER OF PAGES	19a. NAME OF RESPONSIBLE PERSON
a. REPORT	b. ABSTRACT	c. THIS PAGE			USAMRMC
Unclassified	Unclassified	Unclassified	Unclassified	56	19b. TELEPHONE NUMBER *(include area code)*

Table of Contents

1. INTRODUCTION

There are striking population/race disparities in prostate cancer (PCa) risk and survival outcome borne out of current health statistics data. This is particularly evident between African Americans (AA) and their European American (EA) counterparts. Epidemiologic studies have shown that higher mortality and recurrence rates for prostate cancer are still evident in AA men even after adjustment for socioeconomic status, environmental factors and health care access. Thus, it is likely that intrinsic biological differences account for some of the cancer disparities. Our overarching hypothesis is that the biological component of prostate cancer health disparities is due, in part, to population-dependent differential splicing of oncogenes and tumor suppressor genes in cancer specimens. The application of genomic approaches has identified splice variants in AA specimens, but absent in EA specimens, encoding more aggressive oncogenic proteins, thereby producing a more cancerous phenotype.

2. KEYWORDS

Prostate cancer, cancer health disparities, alternative RNA splicing, African American, European American, oncogenes, tumor suppressor genes, phosphatidylinositol-4,5-bisphosphate 3-kinase catalytic subunit delta, fibroblast growth factor receptor 3

3. ACCOMPLISHMENTS

Year 3 goals as stated in SOW:

Specific Aim 1. To define splice variant pairs (AA-specific variant versus EA-counterpart variant) associated with differential oncogenic behavior *in vitro*, and to delineate the mechanism of action.

Task 1. **Full-length cloning and *in vitro* validation of splice variant pairs**. Subtasks will be run concurrently and are as follows:

1a. Full-length cloning of splice variant pairs and ectopic over-expression into PCa cell lines.

1b. *In vitro* validation of differential oncogenic behavior by full-length splice variant pairs. Splice variant pairs (e.g. AA-specific versus EA-counterpart variant of PIK3CD and FGFR3) will be individually over-expressed in the same PCa cell line background, and screened for differential oncogenic behavior.

1c. *In vitro* validation of differential protein/enzyme activity by full-length splice variant pairs. Splice variant pairs will be individually over-expressed into appropriate cell line for enzyme activity assays and/or assessment of downstream activation of cell signaling components. Activation of downstream signaling components by splice variants will be assessed, for example, by measuring phosphorylation of downstream signaling components with phospho-specific antibodies (e.g. phospho-Akt, phospho-ERK, etc.).

Task 2. ***In vitro* screening and full-length cloning of additional splice variant pairs**. Subtasks will be run concurrently and are as follows:

2a. Exon-targeting and splice junction-targeting siRNAs will be used in appropriate PCa cell lines to identify splice variant pairs exhibiting differential oncogenic behavior following knockdown.

2b. From subtask 2a, we will select 5-10 splice variant pairs that exhibited differential oncogenic behavior for full-length cloning and ectopic over-expression in appropriate cell lines.

2c. Cell lines over-expressing individual full-length variant pairs (e.g. AA-specific variant versus EA-counterpart variant) will be validated *in vitro* for differential oncogenic behavior using *in vitro* screens described in subtask 1b. We will also test for differential sensitivity of splice variant pairs to small molecule inhibitors, if available.

2d. Cell lines over-expressing individual variant pairs (e.g. AA-specific variant versus EA-counterpart variant) will be screened *in vitro* for differential protein/enzyme activity and cell signaling as described in subtask 1c. We will also test for differential sensitivity of splice variant pairs to small molecule inhibitors, if available.

Specific Aim 2. To characterize oncogenic differences of splice variant pairs *in vivo* using xenograft animal models.

Task 1. **Validate differential oncogenic behavior of the splice variant pair for PIK3CD *in vivo***. Stably expressed S (AA-specific) or L variants (EA-counterpart) of *PIK3CD* in appropriate cell line(s) will be transplanted ($1x10^6$ to 10^7 cells) into male SCID-NOD immuno-deficient mice for proliferation and metastasis assays.

Task 2. **Validate differential oncogenic behavior of additional splice variant pairings *in vivo.*** We will test *in vivo* an additional 4-9 splice variant pairings defined in Aim 1, Task 1, Subtasks 1b-1c (e.g. one variant pairing could be the AA-specific and EA-counterpart variants for *FGFR3*), or defined in Aim 1, Task 2, Subtasks 2c-2d.

Year 3 major accomplishments include the following:

i. **Manuscript detailing our findings on the oncogenic behavior of the AA-specific/enriched *PIK3CD* short variant (*PIK3CD-S*) compared to the EA *PIK3CD* long variant (*PIK3CD-L*) has been positively reviewed by *Nature Communications***

Assessment of our *Nature Communications* manuscript by the reviewers was positive, albeit they requested a number of additional experiments that have been completed this past month. Our manuscript has been resubmitted. Our additional findings can be summarized as follows:

AA-specific/enriched variant PI3KCD-S is resistant to small molecule inhibitor CAL-101, while EA variant PI3KCD-L is sensitive. In our original *Nature Communications* submission, we had stably over-expressed the *PIK3CD-S* and *PIK3CD-L* variants (individually in the EA PCa cell lines PC-3 and VCaP. These stably transfected cell lines were tested *in vitro* for sensitivity to CAL-101 treatment (**Fig. 1A**). CAL-101 is a PI3Kδ inhibitor in clinical trials for various cancers. PCa cell lines over-expressing the EA *PIK3CD-L* variant exhibited a decrease in the activity of the PI3K/AKT pathway following CAL-101 treatment, as seen by a loss of AKT, mTOR and S6 phosphorylation. Remarkably, the same EA PCa cell lines stably over-expressing equivalent levels of the AA *PIK3CD-S* variant were completely resistant to CAL-101. In other words, there was no significant change in AKT, mTOR and S6 phosphorylation levels before and after CAL-101 treatment.

In cell proliferation assays, we demonstrate that BrdU labeling in VCaP and PC-3 cells over-expressing the EA *PIK3CD-L* variant was inhibited by CAL-101 in a dose-dependent manner, while proliferation of VCaP and PC-3 cells over-expressing the AA *PIK3CD-L* variant were resistant to CAL-101 (**Fig. 1B**).

The reviewers had requested that we assess whether or not cell lines over-expressing the *PIK3CD-S* or *PIK3CD-L* variant exhibited differential sensitivity to inhibitors of downstream signaling components. Interestingly, *PIK3CD-S*- and *PIK3CD-L*-over-expressing cell lines were equally to selective inhibition of AKT with MK-2206 (**Fig. 1C**). These results demonstrate that PI3Kδ-S-stimulated proliferation is resistant to CAL-101 inhibition in sharp contrast to PI3Kδ-L; while inhibition of AKT, which is downstream of PI3Kδ-S, effectively blocked proliferation.

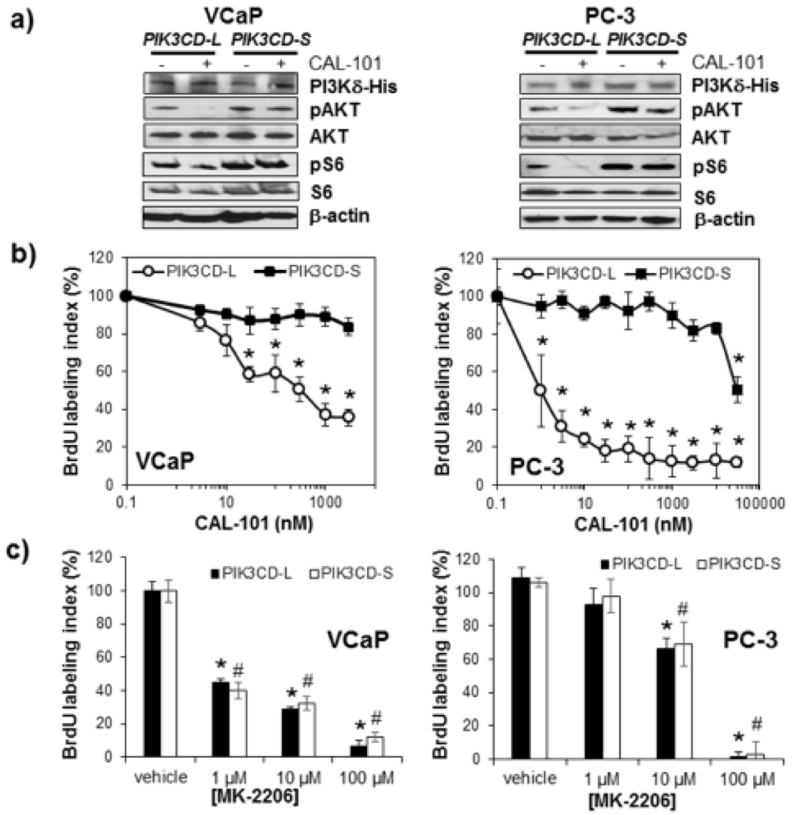

Fig. 1. PI3Kδ-S, but not PI3Kδ-L, is resistant to small molecule inhibition of PI3K/AKT/mTOR signaling and proliferation. (a) Assessment of PI3K/AKT/mTOR signaling following treatment with vehicle (saline) or CAL-101 (100 nM, 24 hrs). PI3K/AKT/mTOR signaling was assessed by western blot analysis with phospho-antibodies to AKT (pAKT) and S6 ribosomal protein (pS6). β-actin served as a loading control. His-tag antibody was used to demonstrate equal expression of His-tagged variant PI3Kδ protein in stably transfected cell lines. Representative images from n = 3-4 independent western blot experiments. *Significantly different from corresponding vehicle control, $P < 0.05$ by ANOVA with Dunnett's post-hoc test. (b) Proliferation in VCaP and PC-3 cells stably overexpressing the *PIK3CD-S* variant or *PIK3CD-L* variant following treatment with vehicle (saline) or selective PI3Kδ small molecule inhibitor CAL-101 (24 hrs), and (c) treatment with vehicle (saline) or selective AKT small molecule inhibitor MK-2206 (24 hrs). Proliferation was assessed using a BrdU labeling assay. Data presented as the mean ± SEM of n=4-6 independent experiments for each treatment group. * or #Significantly different from corresponding vehicle control, $P < 0.05$ by ANOVA with Dunnett's post-hoc test.

ii. Defining mechanism of PI3KCδ-S oncogenecity and resistance to CAL-101 inhibition

Employing cell-free system to define: a) mechanism of increased oncogenecity of PI3KCδ-S over PI3KCδ-L, and b) the mechanism of PI3KCδ-S resistance versus PI3KCδ-L sensitivity to CAL-101 inhibition. A major question that the reviewers of *Nature Communications* required us to address was the mechanism of enhanced PI3KCδ-S oncogenecity and resistance (**Fig. 2**). The result of the exclusion of exon 20 (168 bp) in the *PIK3CD-S* variant is an in-frame deletion of 56 amino acids (residues 810-865) in the catalytic

domain of the PI3Kδ-S isoform (**Fig. 2a**). To gain further insight into the functional differences

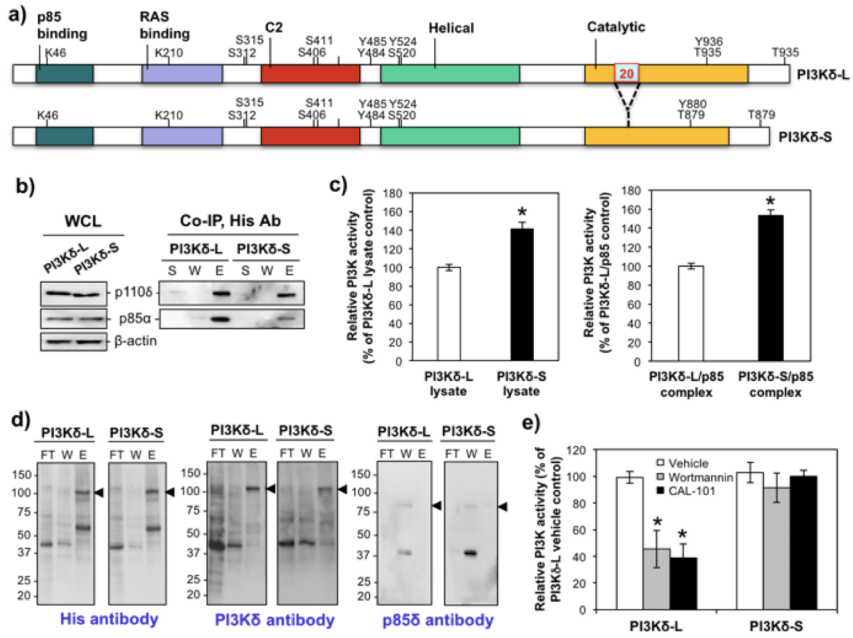

Fig. 2. Cell-free kinase assay of PI3Kδ isoforms and tertiary structure modeling of PIK3δ-small molecule inhibitor interactions. (a) Schematic representation of protein domains of PI3Kδ-L and -S isoforms. Adaptor (p85)-binding, RAS binding, C2, helix and catalytic domains are highlighted. Phosphorylation and ubiquitination sites (S, T, Y and K) and the region encoded by exon 20 (56 amino acids) residing in the catalytic domain are indicated. (b) Co-immunoprecipitation (Co-IP) of PI3Kδ/p85 complex followed by western blot, (c) and PI3K activity assays. S, supernatant; W, wash fraction; E, eluted fraction. Blots are representative of 3-5 similar results. Anti-His antibody was used independent experiments with used in the Co-IP experiments and anti-His, anti-p85α and anti-actin antibodies were used in the western blotting. *Significantly different kinase activities in total lysates of PI3Kδ-S vs. PI3Kδ-L expressing cells, or purified PI3Kδ-S/p85 vs. PI3Kδ-L/p85 complexes. $P < 0.05$ using Student t-test. Data presented as mean ± SEM of n = 4 for each treatment group. (d) Purification of His-tagged PI3Kδ-L and -S isoforms. Western blot analysis of Ni-NTA resin-purified PI3Kδ isoforms from transfected PC-3 cells using His and PI3Kδ antibodies. FT, flow-through; W, wash fraction; E, eluted fraction. Blots are representative of 4 independent experiments with similar results. Closed arrowheads indicate PI3Kδ isoforms. (e) Cell-free kinase assay of L and S isoforms of PI3Kδ in the presence of vehicle (PBS), 100nM wortmannin or 100nM CAL-101. *Significantly different from vehicle control-treated PI3Kδ-L isoform. $P < 0.05$ by ANOVA with Dunnett's post-hoc test. Data presented as mean ± SEM of n = 4-5 for each treatment group.

between PI3Kδ isoforms, the interaction of PI3Kδ-L and -S with regulatory subunit p85α was investigated. Whole cell lysates from PC-3 cells over-expressing either His-tagged PI3Kδ-S or PI3Kδ-L were subjected to western analysis, demonstrating that each cell line expressed equivalent levels of their respective PI3Kδ isoform as well as equal p85α expression (**Fig. 2b**; left panel). Interestingly, co-IP of the PI3Kδ/p85α complex from whole cell lysates using an anti-His antibody demonstrated that p85α bound with 3-4-fold greater proficiency to PI3Kδ-L compared to p85α binding to PI3Kδ-S (**Fig. 2b**; right panel, column E). Binding proficiency was inversely correlated with PI3Kδ isoform kinase activity (**Fig. 2c**; right panel).

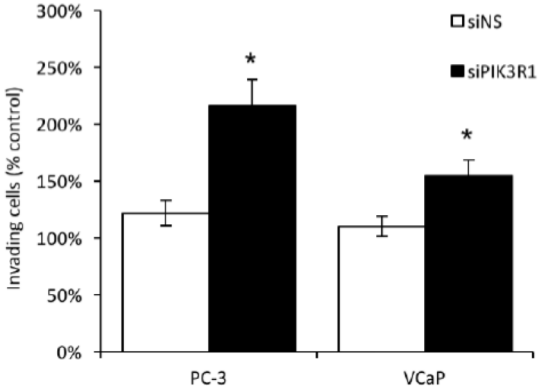

Fig. 3. Knockdown of p85a increases invasive activity of EA PCa cell lines. Invasion was assessed using Matrigel assay following siRNA-mediated knockdown of p85**a** (PIK3R1). SiRNA-SMART pool for targeting PIK3R1 was purchased from Dharmacon (Lafayette, CO). Data presented as the mean ± SEM of n=3-4 independent experiments for each treatment group. *P < 0.05 by ANOVA with Dunnett's post-hoc test. siNS, Nonsense siRNA control.

Next, His-tagged PI3Kδ isoforms were purified from the lysates of PC-3 cells overexpressing either PI3Kδ-S or PI3Kδ-L using Ni-NTA resin columns. As shown in **Fig. 2d** (left and middle panels), purification of the PI3Kδ-S and -L isoforms was verified by western blotting using anti-His or anti-PI3Kδ antibodies. In addition, the Ni-NTA resin column purification approach resulted in the isolation of PI3Kδ isoforms that were no longer bound to p85α (**Fig. 2d**; far right panel, column E). The purified PI3Kδ isoforms (minus p85α) were incubated with vehicle, non-selective PI3K inhibitor wortmannin (100 nM) or PI3Kδ-specific inhibitor CAL-101 (100 nM), and subjected to a PI3K activity assay. In the absence of bound p85α, kinase activity of PI3Kδ-L was equivalent to PI3Kδ-S (**Fig. 2e**, compare vehicle treatments). In agreement, siRNA-mediated knockdown of p85α in wild-type EA PCa cell lines VCaP and PC-3 was associated with an increase in invasive activity (**Fig. 3**). Remarkably, wortmannin and CAL-101 significantly inhibited the activity of the PI3Kδ-L isoform, but not the PI3Kδ-S isoform (**Fig. 2e**). These results demonstrate that PI3Kδ-S maintains kinase activity even in the presence of small molecule inhibitors, supporting our earlier *in-vitro* and *in-vivo* results presented in our Year 2 progress report.

iii. We have determined that high *PI3KCD-S* and *FGFR3-S* expression is associated with poorer patient prognosis

We have performed survival analysis of The Cancer Genome Atlas (TCGA) RNA-Seq data, demonstrating that either high expression of *PIK3CD-S* or *FGFR3-S* associates with significantly poorer survival in PCa patients (**Fig. 4**), demonstrating further the potential relevance of these two short variants in PCa.

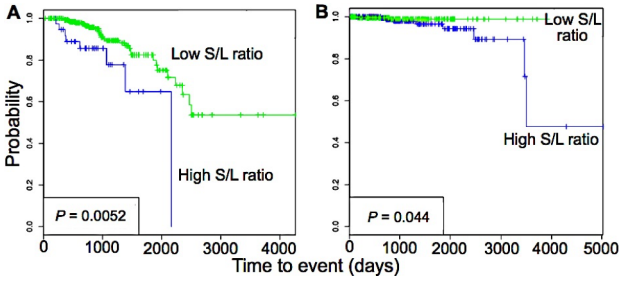

Fig. 4. PIK3CD-S (A) and FGFR3-S (B) are associated with decreased survival among PCa patients. RNA-Seq and disease free survival data for PCa (n = 494 patients) was obtained from The Cancer Genome Atlas (TCGA) (https://tcga-data.nci.nih.gov). P-values for survival curves determined by the log-rank test.

Year 3 opportunities for training and professional development:

AACR Health Disparities Presentation. Year 3 of this proposal has provided hands-on training for PhD graduate student Jacqueline Olender. The PI is serving as Ms. Olender's mentor and she has participated in both the *in vitro* and *in vivo* work described herein. This work is part of Ms. Olender's PhD dissertation research project. An NIH/AACR Scholar-in-Training Award was awarded to Ms. Olender to present her thesis work entitled, "Alternative splicing of FGFR3 as a mechanism for prostate cancer health disparities" at the 9th AACR Conference on The Science of Cancer Health Disparities in Racial/Ethnic Minorities and the Medically Underserved.

Dissemination of results and outreach to communities of interest:

Mentoring. During Year 3 of this grant, my lab has mentored 4 medical students (Lauren Simpkins, Daniel Szvarca, Breeana Johnq, Erin Good) during the summer of 2016, on various PCa disparities-related research projects. under the supervision of myself and Dr. Wang.

Invited Presentation. This work was presented at the June 2016, Khon Kaen University Cancer Summit Meeting in Khon Kaen, Thailand. "Aberrant Alternative Splicing of mRNA as a Mechanism in Prostate Cancer Disparities", Lee N.H.

Goals for next reporting period:

None to report

4. IMPACT

Impact on the development of the principal discipline(s) of the project:

Principal discipline -- Understanding prostate cancer biology and disparities. Taken together, our *in vitro* and *in vivo* research on AA-specific/enriched *PIK3CD-S* and *FGFR3-S* variants provide strong evidence that differential splicing may play a critical role in PCa health disparities. Our future goal is to identify the underlying molecular mechanism(s) responsible for the differential splicing events observed in AA versus EA PCa specimens.

Impact on other disciplines:

Other disciplines -- Our work demonstrates that the short variant encodes a more aggressive oncogenic signaling protein isoform, PI3Kδ-S, that is resistant to small molecule inhibitor idelalisib as defined by *in vitro* assays and mouse xenograft models. In contrast, the corresponding EA isoform (PI3Kδ-L) encodes a less aggressive isoform that is sensitive to idelalisib inhibition. Our discovery portends a genetic screening test for cancer patients that may be resistant to idelalisib therapy, which is particularly germane in hematologic malignancies. Idelalisib is FDA approved for relapsed chronic lymphocytic leukemia and relapsed non-Hodgkin lymphoma. Treatment resistance is observed in ~30-40% of patients, and the mechanism of resistance is currently unknown. Our hypothesis is that the short mRNA variant of *PIK3CD* may be playing a major role in treatment resistance. Clinical and molecular studies are currently underway to test this hypothesis.

Impact on technology transfer:

Our findings that the AA PIK3CD-S variant protein is resistant to CAL-101 has sparked interests in companies that are investigating small molecule inhibitors of kinases involved in cancer progression. These companies are gaining an appreciation that alternative splicing in kinases can affect the sensitivity these signaling proteins to cancer therapeutic agents. Our findings highlights the potential importance of prescreening patients for their variant protein in order to prognosticate whether a particular small molecule inhibitor will be therapeutically efficacious.

Impact on society beyond science and technology:

Nothing to report

5. CHANGES/PROBLEMS

Changes in approach:

None

Actual or anticipated problems or delays:

None

Changes that had significant impact on expenditures:

None

Significant changes in use or care of human subjects, vertebrate animals, biohazards, and/or select agents:

None

6. PRODUCTS

Publications, conference papers, and presentations:

i. Manuscript in review. Wang B.-D., Ceniccola K., Hwang S., Andrawis R., Horvath A., Freeman J.A., Knapp S., Ching T., Garmire L., Patel V., Garcia-Blanco M.A., Patierno S.R. and Lee N.H. (2016) Aberrant alternative splicing in African American prostate cancer: novel driver of tumor aggressiveness and drug resistance. ***Nature Commun.*** (positively reviewed by reviewers; have completed requested experiments and resubmitted).

ii. Presentation "Alternative splicing of FGFR3 as a mechanism for prostate cancer health disparities" at the 9th AACR Conference on The Science of Cancer Health Disparities in Racial/Ethnic Minorities and the Medically Underserved, September 25 - 28, 2016.

iii. Manuscript in review. Freedman JA, Wang Y, Xuechan L, Liu H, Moorman P, George DJ, Lee NH, Hyslop T, Wei Q and Patierno S (2016) Single nucleotide polymorphisms of stemness pathway genes predicted to regulate RNA splicing, microRNA and transcription are associated with prostate cancer survival. ***Clinical Cancer Res.*** (submitted)

iv. Manuscript in review. Wang Y, Freedman JA, Liu H, Moorman P, Hyslop T, George DJ, Lee NH, Patierno S and Wei Q (2016) Variants of stemness-related genes predicted to regulate RNA splicing associated with racial disparities in susceptibility to prostate cancer. ***Carcinogenesis*** (submitted)

Website(s) or other Internet site(s):

None

Technologies or techniques:

None

Inventions, patent applications, and/or licenses:

i. Our provisional patent application has been issued. Application number: 61/948,218. Date patent issued: 09/27/16. Application title: Companion Diagnostics for Cancer and Screening Methods to Identify Companion Diagnostics for Cancer Based on Splicing Variants

Other Products:

None

7. PARTICIPANTS & OTHER COLLABORATORS

Individuals working on this project:

Name:	Norman H Lee, PhD
Project Role:	PI
Nearest person month worked:	3
Contribution to project:	Direct and oversee entire project. Involved in experimental design and statistical analysis.

Name:	Bi-Dar Wang, PhD
Project Role:	Co-Investigator
Nearest person month worked:	3
Contribution to project:	Contributed to the cloning of variant cDNAs, in vitro, xenograft assays and cell-free protein purification and analysis.
Funding support:	Partially supported by GWU bridge support

Name:	Jacqueline Olender
Project Role:	PhD graduate student
Nearest person month worked:	12
Contribution to project:	Contributed to the cloning of variant cDNAs, in vitro and in vivo assays

Name:	Patricia Latham, MD
Project Role:	Co-Investigator
Nearest person month worked:	1
Contribution to project:	Animal necropsy and immunohistochemistry of xenografts

Change in the active other support of the PD/PI(s) or senior/key personnel since the last reporting period:

None

Other organizations were involved as partners:

Nothing to report

8. SPECIAL REPORTING REQUIREMENTS

Nothing to report

9. APPENDICES

i. Wang B.-D., Ceniccola K., Hwang S., Andrawis R., Horvath A., Freeman J.A., Knapp S., Ching T., Garmire L., Patel V., Garcia-Blanco M.A., Patierno S.R. and Lee N.H. (2016) Aberrant alternative splicing in African American prostate cancer: novel driver of tumor aggressiveness and drug resistance. ***Nature Commun.*** (positively reviewed by reviewers; have completed requested experiments and resubmitted). Part of the published work was supported by W81XWH-13-1-0449.

Aberrant Alternative Splicing in African American Prostate Cancer: novel driver of tumor aggressiveness and drug resistance

Bi-Dar Wang, Kristin Ceniccola, SuJin Hwang, Ramez Andrawis, Anelia Horvath, Jennifer A. Freeman, Jacqueline Olender, Stefan Knapp, Travers Ching, Lana Garmire, Vyomesh Patel, Mariano A. Garcia-Blanco, Steven R. Patierno, and Norman H. Lee

Author information

Affiliations

Department of Pharmacology and Physiology, School of Medicine and Health Sciences, The George Washington University, Washington, District of Columbia 20037, USA.
Bi-Dar Wang, Kristin Ceniccola, Anelia Horvath, Jacqueline Olender & Norman H. Lee

Department of Pharmaceutical Sciences, School of Pharmacy and Health Professions, University of Maryland Eastern Shore, Princess Anne, Maryland 21853, USA.
Bi-Dar Wang

Department of Microbiology, Immunology and Tropical Medicine, School of Medicine and Health Sciences, The George Washington University, Washington, District of Columbia 20037, USA.
SuJin Hwang

Duke Cancer Institute, Duke University Medical Center, Durham, North Carolina 27710, USA.
Jennifer A. Freeman & Steven R. Patierno

Department of Clinical Pharmacology, University of Oxford, Oxford, UK, and the Nuffield Department of Clinical Medicine, Structural Genomics Consortium, University of Oxford, Oxford OX3 7BN, UK.
Stefan Knapp

Cancer Epidemiology Program, University of Hawaii Cancer Center, Honolulu, Hawaii 96813, USA
Travers Ching & Lana Garmire

Department of Biochemistry & Molecular Biology, The University of Texas Medical Branch at Galveston, Galveston, Texas 77555, USA
Mariano A. Garcia-Blanco

Oral and Pharyngeal Cancer Branch, National Institute of Dental and Craniofacial Research, National Institutes of Health, Bethesda, Maryland 20892, USA.
Vyomesh Patel

Contributions
B.-D.W. and N.H.L. conceived and designed the study. B.-D.W. and J.O. performed the microarray experiments, tissue sample analysis and in-vitro assays, B.-D.W., V.P., K.C. and S.H. were involved in animal work, R.A. collected clinical samples for the study, B.-D.W., N.H.L., A.H., T.C., L.G. and M.A.G.-B. carried out genomic data analysis. B.-D.W. and S.K. performed 3D modeling of protein isoforms. B.-D.W., N.H.L, J.A.F. and S.R.P. wrote the manuscript with input from all authors. N.H.L. supervised the project.

Competing financial interests
The authors declare no competing financial interests

Corresponding Author
Correspondence to: Norman H. Lee

Abstract

Despite the current clinical challenge of reducing prostate cancer (PCa) disparities, molecular mechanisms contributing to race-related tumor aggressiveness have not been fully characterized and the RNA splicing landscape of PCa across racial populations has not been explored. Here, we identify novel genome-wide, race-related RNA splicing events as critical mechanisms driving PCa aggressiveness and therapeutic resistance in African American (AA) men. AA-enriched splice variants of *PIK3CD*, *FGFR3*, *TSC2* and *RASGRP2* contribute to greater oncogenic potential compared to corresponding European American (EA)-expressing variants. Ectopic overexpression of the newly cloned AA-enriched variant, *PIK3CD-S*, in EA PCa cell lines enhances AKT/mTOR signaling and increases proliferative and invasive capacity *in vitro* and confers resistance to selective PI3Kδ inhibitor, CAL-101, in mouse xenograft models. High *PIK3CD-S* expression in PCa specimens associates with poor survival. These results highlight the potential of RNA splice variants to serve as novel biomarkers and molecular targets for developmental therapeutics in aggressive PCa.

Introduction

Prostate cancer (PCa) is the most commonly diagnosed cancer and the second leading cause of cancer death among American men [1]. Striking population disparities in PCa risk and clinical outcome have been observed across racial and ethnic groups. Notably, African American (AA) men exhibit 1.6-fold higher incidence and 2.4-fold higher mortality rates of PCa compared to European American (EA) men [2,3]. Socioeconomic factors remain a major component accounting for the PCa disparities between AA and EA populations. However, higher mortality and recurrence rates are still observed in AA PCa even after adjustment of the socioeconomic factors between AAs and EAs [4,5], suggesting that intrinsic differences in the biological characteristics and genomic composition of AA and EA PCa may also play a critical contributing role in PCa disparities among racial groups.

Alternative splicing is a post-transcriptional process that occurs during the maturation of mRNA transcripts, allowing the synthesis of alternative mRNA transcripts that encode structurally and perhaps functionally disparate protein isoforms. Next-generation DNA and RNA sequencing (NSG) data suggests that more than 90% of human genes undergo alternative splicing [6], and the resulting complexity in the mRNA transcriptome explains how ~20,000 human protein-coding genes in the genome can lead to the diversity of >250,000 distinct proteins in the proteome. Accumulating evidence indicates that alternative and/or aberrant splicing of precursor (pre)-mRNA also plays an important but largely underappreciated role in human cancers [7,8], including PCa pathogenesis [9]. For example, the B-cell lymphoma 2-like 1 (*BCL2L1*) pre-mRNA is alternatively spliced into two variants, *Bcl-xS* and *Bcl-xL*, encoding protein isoforms with opposite biological effects. Bcl-xS is a pro-apoptotic protein, while BcL-xL has anti-apoptotic properties that confer resistance to

chemotherapeutic agents in PCa cell line PC-3 [10]. The fibroblast growth factor receptor 2 (*FGFR2*) pre-mRNA also undergoes alternative splicing, where *FGFR2-IIIb* is predominately expressed in epithelial cells and *FGFR2-IIIc* is primarily associated with mesenchymal cells and epithelial-to-mesenchymal transition of prostate tumor cells [11]. Another example is the *TMPRSS2-ERG* gene fusion commonly found in PCa and associated with poor clinical outcome [12-14]. In a comparative study of *TMPRSS2-ERG* variants ectopically overexpressed in primary prostatic epithelial cells, variants containing exon 8 were associated with increased cell proliferation, invasion and motility [15]. The androgen receptor (AR) signaling pathway is critically associated with growth and survival in PCa [16]. Aberrant/alternative splice variant *AR-V7* is overexpressed in the hormone-refractory PCa, being correlated with poor survival and higher recurrence rates following surgical treatment [17]. Finally, extensive unspliced pre-mRNAs have been observed in metastatic castration-resistant PCa [18].

Despite the significance of alternative and/or aberrant splicing in PCa development and progression irrespective of race, the occurrence of race-specific/-enriched (AA vs. EA) PCa splicing events and a causal relationship between these events and observed PCa health disparities among racial groups remains unexplored. For example, it is unclear if *FGFR2-IIIc*, *TMPRSS2-ERG* variants containing a 72-base exon, *AR-V7* and/or other as yet undiscovered variants associated with more aggressive PCa might be predominantly or selectively expressed in AA PCa, thus possibly contributing to the PCa disparities. In addition, it is unknown if differences in mRNA splicing along racial/population lines occur in only a limited number of genes or more globally across the transcriptome. If the latter, it will be important to ascertain whether these genome-wide, differential splicing events are over-

represented within specific gene ontologies (i.e. proto-oncogenes, tumor suppressor genes and/or signaling pathways playing roles in particular biological processes). Lastly, if present, assessment of the functional consequences of any race-specific (or -enriched) splicing events will provide critical further insight into the genetic/molecular mechanisms underlying PCa disparities among racial groups. To this end, we have applied a functional genomics approach to address these questions in biopsy and surgical samples of AA and EA prostate cancer. We demonstrate global differential splicing events involving >2,500 genes in prostate tumors of AA versus EA. The vast majority of genes exhibiting race-specific/-enriched differential splicing are associated with cancer and computational analysis identified >25 cancer-related pathways with an over-representation of differential splicing events. Moreover, we have evaluated the biological significance of these splicing events in a subset of proto-oncogenes and identified and cloned a novel AA-enriched *PIK3CD* short variant (*PIK3CD-S*) that imparts increased proliferative and invasive properties to PCa cell lines compared to an EA-expressing long variant (*PIK3CD-L*). Using xenograft and metastasis mouse models, we found that *PIK3CD-S* encodes an isoform that is resistant to small molecule inhibitors targeting PIK3CD, while the variant encoded by *PIK3CD-L* is sensitive to such inhibitors. These results highlight an opportunity to utilize population level differences in tumor biology to: i) discover novel splice variants that will likely serve as novel precision biomarkers and/or molecular targets for developmental therapeutics against aggressive PCa (particularly in the AA population), ii) identify previously hidden splice variants encoding oncogenic signaling proteins resistant to small molecule inhibitors, and iii) assimilate splice variant information for prognostication of cancer aggressiveness and/or therapeutic responsiveness.

Results

Exon array analysis reveals genome-wide differential splicing events in AA versus EA PCa. A total of 35 PCa (20 AA, 15 EA) and 35 patient-matched normal prostate (NP) specimens (20 AA, 15 EA) derived from chemo-/hormone-/radiation-naïve patients were interrogated using the Affymetrix Human Exon 1.0 ST GeneChip to assess differential splicing (DS) events. Gleason scores of PCa specimens (range 6-8) and patient ages (range 49-81 years) were not significantly different between the AA and EA cohorts (P>0.05 Fisher's exact test). In AA PCa vs. EA PCa and AA NP vs. EA NP, the significant differentially expressed exons (**Figs. 1a** and **1b**) could be modeled using the Alternative Splice ANOVA approach [19] into 2,520 and 2,849 DS events, respectively (**Supplementary Table S1**, **Supplementary Fig. S1**). As depicted in the Venn diagram (**Fig. 1c**), 1,876 genes (i.e. 2,520 - 644) exhibited DS events unique to AA PCa vs. EA PCa, 2,205 differentially spliced genes (i.e. 2,849 - 644) were unique to AA NP vs. EA NP and 644 DS events were in common (i.e. DS events pre-existing in AA NP vs. EA NP and preserved in AA PCa vs. EA PCa). Examples of genes with pre-existing DS events included *PIK3CD*, *ITGA4* and *MET*, while *RASGRP2*, *NF1* and *BAK1* are examples of differentially spliced genes occurring only in AA PCa vs. EA PCa. In EA PCa vs. EA NP and AA PCa vs. AA NP, the significant differentially expressed exons (**Supplementary Fig. S2**) could be modeled into 1,297 and 1,733 DS events, respectively (**Fig. 1c**). Presumably, a subset of 1,575 genes (i.e. 1,733 - 158) with DS events unique to AA PCa may contribute to PCa disparities. Examples in this category included *FGFR3* and *TSC2* (**Supplementary Table S1**). On the other hand, a subset of 158 genes with DS events in common to both AA and EA PCa may contribute to PCa progression regardless of

race (**Fig. 1c**). Consistently, such genes included *TMPRSS2* and *AR* (**Supplementary Table S1C and D**). Analysis of the exon array data employing both gene-wise [20,21] and Alternative Splice ANOVA modeling approaches [19] identified 898 genes (i.e. 1,188 - 290) that were differentially expressed but not exhibiting DS in AA PCa vs. EA PCa, and 2,230 (i.e. 2,520 - 290) genes undergoing DS but not differential expression (e.g. level of variant 'A' for gene 'X' in AA PCa equivalent to variant 'B' for gene 'X' in EA PCa; **Fig. 1c**).

Prevalence of differential splicing events in cancer-associated pathways. We categorized genes undergoing DS in AA PCa vs. EA PCa based on molecular function, gene ontology (GO) and disease association. Relevant cancer-related ontologies included cell growth and proliferation, cell death and survival, cellular movement, cell adhesion and DNA damage/repair (*P*-value ranged from 6.54×10^{-12}-1.88×10^{-2}; **Supplementary Table S2**). Notably, a large fraction (1,816 out of 2,520, 71.8%) of the differentially spliced genes were discovered to be over-represented across multiple cancers, including gastrointestinal, colorectal, renal, breast, brain, rectal, brain, lung, stomach, prostate and hematologic cancers (*P*-values ranged from 1.43×10^{-9}-1.96×10^{-2}; **Fig. 1d** and **Supplementary Table S2**). There was an unexpected skewing in the distribution of in-frame versus out-of-frame exon skipping events in cancer-related genes, where in-frame events were significantly favored in AA over EA PCa specimens ($P < 0.05$ Fisher's exact test; **Supplementary Table S3**). This finding was in line with an overall significant preference for in-frame events across all genes (cancer-related and non-cancer-related) in AA PCa specimens (**Supplementary Table S3**). In the case of non-cancer-related genes only, there was

no significant skewing of in-frame distribution events between AA versus EA PCa (**Supplementary Table S3**).

We also examined the distribution of DS events across cell signaling pathways. There was a striking significant over-representation of DS events in multiple oncogenic signaling pathways, including EGF, VEGF, PTEN, PI3K/AKT, ERK/MAPK, cell cycle and NFκB signaling (Fisher's Exact Test, *P*-values of 0.00126, 0.00891, 0.00426, 0.01288, 0.01622, 0.01259 and 0.02089, respectively; **Supplementary Fig. S3** and **Supplementary Table S4**). Interestingly, many of these same pathways are known to be mutated based on earlier cancer genome sequencing studies [22-24]. A composite oncogenic signaling pathway comprised of DS events found in AA PCa vs. EA PCa is depicted in **Fig 2**. Taken together, our data provide strong evidence that DS events may play a critical role in PCa disparities.

Validation of alternative splice variants in AA vs EA PCa. We proceeded to validate a subset of both proto-oncogenes and tumor suppressor genes with DS events in our composite cancer signaling pathway, including *PIK3CD*, *FGFR3*, *TSC2, ITGA4*, *MET*, *NF1*, *BAK1, ATM* and *RASGRP2* (**Fig. 2**). RT-PCR was performed on RNA samples obtained from AA and EA PCa specimens originally interrogated by the exon arrays. Primer pairs or trios were designed for RT-PCR to amplify simultaneously multiple variants of each gene (**Fig. 3a**). As shown in **Fig. 3b**, AA PCa specimens contained both *PIK3CD* long (*PIK3CD-L*, including exon 20) and short (*PIK3CD-S*, missing exon 20) variants, whereas EA PCa samples predominately expressed the *PIK3CD-L* variant. Hence, the RT-PCR results were in agreement with the exon array data, indicating the presence of an AA-enriched *PIK3CD-S* variant. Analogous findings were obtained where either a short or long variant of each gene

was confirmed by RT-PCR to be enriched or uniquely expressed in AA (*TSC2-S, ITGA4-L*, *MET-L*, *BAK1-L*) or EA PCa specimens (*FGFR3-L, ITGA4-S*, *MET-S*, *NF1-S*, *BAK1-S*) (**Fig. 3b**; see **Supplementary Fig. S4** for quantitative RT-PCR results from n = 22-25 AA and n = 21-24 EA PCa specimens). Exon array data also revealed two alternative *RASGRP2* transcripts with apparent mutually exclusive exon skipping events (**Fig. 3a** and **Supplementary Fig. S1d**). RT-PCR validation likewise confirmed that a *RASGRP2-b* variant (exon 11 excluded) was exclusively expressed in AA PCa, while a *RASGRP2-a* variant (exon 12 excluded) was enriched in EA PCa (**Fig. 3b** and **Supplementary Fig. S4**). We were unable to validate differential splicing of *ATM*, whereas 2 additional genes (*GSK3A* and *EPHA1*) identified by exon arrays as not undergoing differential splicing were confirmed by RT-PCR. In summary, there was strong agreement (10/11 or 91%) between exon array and RT-PCR results, thus providing an internal quality metric to our global analysis of differential splicing events between AA and EA PCa (see Supplemental Materials & Methods for additional metrics).

The race-dependent expression of *PIK3CD* variants was particularly interesting owing to recent findings implicating PI3Kδ (p110δ) kinase activity in hematologic malignancies as well as other cancer types [25-28]. In a separate cohort of PCa specimens obtained from 32 AAs (age range 52-76 years, Gleason score range 6-8) and 30 EAs (age range 50-82 years, Gleason score range 6-8; not significantly different from AA, Fisher's exact test, P>0.05), quantitative RT-PCR validation was performed reaffirming significantly higher levels of *PIK3CD-S* relative to *PIK3CD-L* in AA compared to EA PCa specimens (**Fig. 3c**). Given the robustness and potential significance of these findings, subsequent *in vitro* and *in vivo* studies centered on the *PIK3CD* variants, as described below.

Molecular cloning of *PIK3CD* splice variants. The AA-enriched *PIK3CD-S* variant has never before been described in the literature nor the UCSC (genome.ucsc.edu/) or Ensembl Genome Browser (www.ensembl.org/). Consequently, we cloned the full-length version of the *PIK3CD-S* variant from the AA PCa cell line MDA PCa 2b and *PIK3CD-L* variant from MDA PCa 2b as well as EA PCa cell lines VCaP and LNCaP using standard molecular approaches (e.g. 5'- and 3'-RACE; see [29]). We likewise cloned matching *PIK3CD-S* and *PIK3CD-L* variants from PCa patient specimens. **Supplementary Fig. S5** schematically depicts the full-length clones of the *PIK3CD-L* variant (comprising a total of 24 exons) along with three different AA *PIK3CD-S* variants (variant excluding exon 8, variant excluding exon 20 and variant excluding both exons 8 and 20) and one AA large deletion variant of the *PIK3CD* gene. Interestingly, exclusion of exon 8 eliminates a 30 amino acid segment situated between the Ras-binding and C2 domains, while exclusion of exon 20 deletes a 56 amino acid segment located in the catalytic domain of PI3Kδ. In subsequent functional studies involving ectopic overexpression of the short variant (see below), we concentrated our efforts on the variant missing exon 20 given the possibility that kinase activity may be affected.

Enrichment of *PIK3CD-S* isoform is associated with enhanced invasive and proliferative phenotypes in AA PCa cells. We hypothesized that the splice variants specific or enriched in AA PCa may contribute to a more aggressive oncogenic phenotype. To test this, we designed both exon-specific and exon junction-specific siRNAs to target either the *PIK3CD-L* or *PIK3CD-S* variant, respectively, in EA and AA PCa cell lines and examined the functional consequences of these knockdowns on

both cell proliferation and invasion. A similar strategy was applied to investigate the biological significance of the variants of *FGFR3*, *TSC2* and *RASGRP2*. VCaP and MDA PCa 2b cell lines were used as population-specific PCa models, as these two cell lines represent bone metastases derived from castration-resistant EA and AA PCa patients, respectively [30,31]. Transfection of VCaP cells with exon 20-specific siRNA (siP_{20}) successfully knocked-down *PIK3CD-L* expression by >8-fold compared to nonsense (ns) siRNA (see **Fig. 4a**, left panel), resulting in a significant loss of proliferative and invasive function in VCaP cells (**Fig. 4b**, left). Conversely, in MDA PCa 2b cells, a >5-fold knockdown of *PIK3CD-L* increased the ratio of *PIK3CD-S/PIK3CD-L* expression by nearly 2-fold (**Fig. 4a**, right panel; see 1.88 *S/L* ratio for ns- versus 3.46 *S/L* ratio for siP_{20}-transfected cells), and this 'enrichment' of the AA-enriched *PIK3CD-S* variant subsequently enhanced proliferation and invasion of the AA cell line (**Fig. 4a**, right panel). Moreover, MDA PCa 2b cells exhibited significantly higher basal invasive and proliferative capacities compared to VCaP cells (see proliferation and invasion of siNS-transfected MDA PCa 2b vs. siNS-transfected VCaP; **Fig. 4b**, left and right panels). To further evaluate the functional impact of *PIK3CD-S* expression on cell proliferation and invasion, the EA and AA PCa cell lines were transfected with siP_j (siRNA specifically targeting the junction sequence exons 19 and 21). Transfection of siP_j had no effect on VCaP proliferation and invasion, as expected since this EA line does not significantly express *PIK3CD-S* (**Figs. 4a** and **4b**, right panels). Upon the transfection of MDA PCa 2b cells with siP_j, *PIK3CD-S* expression was significantly knocked-down (**Fig. 4a**, right), resulting in a loss of cell proliferation and invasion (**Fig. 4b**, right). Taken together, these results suggest that *PIK3CD-S* is the more aggressive variant, promoting PCa proliferation and invasion to a greater extent than *PIK3CD-L*.

Several additional exon-specific siRNAs were designed to test whether other AA-specific/-enriched splice variants also functionally contribute to greater PCa aggressiveness. SiRNAs targeting exon 14 (*siFGFR3-ex14*), exon 20 (*siTSC2-ex20*) and exon 11 (*siRASGRP2-ex11*) were used to selectively suppress expression of *FGFR3-L*, *TSC2-L* and *RASGRP2-a* splice variants (predominately expressed in EA), respectively. Upon siRNA-mediated knockdown of *FGFR3-L*, *TSC2-L* or *RASGRP2-a* (**Supplementary Figs. S6a-c**, top panels) in MDA PCa 2b cells, the expression ratios of *FGFR3-S/FGFR-L*, *TSC2-S/TSC2-L* and *RASGRP2-b/RASGRP2-a* increased and correlated with augmented invasive and/or proliferative capacity of the AA-derived MDA PCa 2b cells (**Supplementary Figs. S6a-c**, bottom panels). Collectively, our *in-vitro* studies strongly suggest that the AA-enriched splice variants *PIK3CD-S*, *FGFR3-S*, *TSC2-S* and *RASGRP2-b* promote PCa aggressiveness.

***PIK3CD-S* isoform promotes activation of AKT/mTOR signaling.** As PI3K plays a central role in the PI3K/AKT/mTOR signaling pathway, we examined the ability of the alternative PI3Kδ isoforms (encoded by the *PIK3CD-L* and *PIK3CD-S* splice variants) to activate down-stream signaling components within this pathway. SiRNA (siP_{20})-mediated knockdown of *PIK3K-L* expression (confirmed by qRT-PCR) led to a drastic decrease in AKT phosphorylation at Thr308 and Ser473 while moderately decreasing (~2-fold) phosphorylation of mTOR in EA cell line VCaP (**Fig. 4c**, top panel). In contrast, knockdown of *PIK3CD-L* in AA MDA PCa 2b cells (resulting in an increased *PIK3CD-S/-L* ratio confirmed by qRT-PCR) led to a sizable increase (2-3-fold) in phosphorylation of AKT, mTOR and S6 (**Fig. 4c**, top panel).

In parallel experiments, siRNA (siP_j)-mediated knockdown of *PIK3K-S* expression (confirmed by qRT-PCR) in MDA PCa 2b cells resulted in a drastic

decrease in the phosphorylation status of AKT, mTOR and ribosomal protein S6 (**Fig. 4c**, bottom panel). As expected, treatment of VCaP cells with the siRNA siP_j had negligible effects on AKT, mTOR and ribosomal protein S6 phosphorylation, as this EA line does not significantly express *PIK3CD-S*. Taken together, the distinct phosphorylation patterns of AKT, mTOR and ribosomal protein S6 in AA and EA PCa cell lines upon selective knockdown of either *PIK3CD-L* or *PIK3CD-S,* again suggested that *PIK3CD-S* is the more aggressive variant, promoting oncogenic signaling.

PI3Kδ-L and PI3Kδ-S isoforms exhibit differential response to small molecule inhibitors *in vitro* and in mouse xenograft and metastasis models. We tested whether pharmacological inhibition of PI3Kδ isoforms represented a potential strategy for ameliorating PCa aggressiveness. CAL-101, a small molecule inhibitor (SMI) specific for PI3Kδ [32-34], was employed to assess its inhibitory effects on oncogenic signaling and proliferation in EA PCa cell lines VCaP and PC-3 that stably overexpressed the His-tagged PI3Kδ-S (excluding exon 20) or PI3Kδ-L isoform (including exon 20). Equivalent levels of PI3Kδ isoform expression in each cell line was confirmed by western blot with a His tag antibody (**Fig. 5a**). In both EA PCa cell lines, ectopic overexpression of PI3Kδ-S was associated with a 2-3 fold greater phosphorylation of AKT and ribosomal protein S6 compared to ectopic overexpression of PI3Kδ-L (**Fig. 5a**, absence of CAL-101 treatment). CAL-101 (50mg/kg) induced a significant reduction in basal AKT and ribosomal protein S6 phosphorylation (**Fig. 5a**) and a dose-dependent inhibition of proliferation in both EA cell lines overexpressing the PI3Kδ-L variant (**Fig. 5b**). In contrast, CAL-101 (50mg/kg) had negligible effects on inhibiting basal AKT signaling in EA PCa cell

lines overexpressing PI3Kδ-S, as phosphorylation states of AKT and ribosomal protein S6 were comparable to vehicle treated cells (**Fig. 5a**). In agreement, BrdU labeling assays demonstrated that proliferation of VCaP and PC-3 cells ectopically overexpressing PI3Kδ-S was greater than cells overexpressing PI3Kδ-L (**Supplementary Fig. S7**). Moreover, PI3Kδ-S-overexpressing VCaP and PC-3 cells were not effectively inhibited by CAL-101 treatment; only at extreme doses of CAL-101 (≥30μM) was proliferative activity in PC-3 cells significantly impaired (**Fig. 5b**). In contrast, the AKT inhibitor MK-2206 [35] dose-dependently decreased proliferation in both PI3Kδ-S- and PI3Kδ-L-overexpressing VCaP and PC-3 cells (**Fig. 5c**). These results suggest that PI3Kδ-S-stimulated proliferation is resistant to CAL-101 inhibition in sharp contrast to PI3Kδ-L; while inhibition of AKT, which is downstream of PI3Kδ-S, effectively blocked proliferation.

To examine the effects of *PIK3CD* splice variants on tumor growth *in vivo*, we subcutaneously injected 2×10^6 PC-3 cells stably overexpressing equivalent amounts of the PI3Kδ-L or PI3Kδ-S (missing exon 20) isoform into the left hind flank of NOD-SCID mice. Mice harboring PI3Kδ-L-expressing or PI3Kδ-S-expressing PC-3 cell xenografts were administrated either vehicle (PBS) or CAL-101 (50 mg/kg) by daily i.p. injection. CAL-101 treatment for 30 days significantly reduced the growth of PI3Kδ-L-expressing xenografts compared to the vehicle treatment (**Figs. 6a** and **6b**). In contrast, mice with xenografts of PI3Kδ-S-expressing cells had negligible suppression of their xenograft growth following CAL-101 treatment compared to vehicle-treated animals (**Figs. 6a** and **6b**).

We further examined the inhibitory effects of CAL-101 on PI3Kδ isoforms in an *in vivo* tumor metastasis model. 1×10^6 *PIK3CD-L*- or *PIK3CD-S*-overexpressing PC-3 cells were injected into the tail-vein of NOD-SCID mice, and animals were

subsequently administrated with vehicle or CAL-101 (50mg/kg) via i.p. injection (3 times per week). After 8 weeks, vehicle-treated mice carrying PI3Kδ-L-overexpressing cells developed prominent tumor metastases in the lungs (**Fig. 6c** and **6d**), while the CAL-101 treatment group exhibited a >50% reduction ($P < 0.05$) of metastases (**Figs. 6c** and **6d**). By comparison, CAL-101 treatment failed to significantly inhibit tumor metastases in mice harboring PI3Kδ-S-expressing cells (**Figs. 6c** and **6d**). Noteworthy, the size of lung metastases (average area of nodules) in mice harboring PI3Kδ-S-overexpressing cells was slightly greater (~15%) compared to animals with PI3Kδ-L-overexpressing cells, albeit not statistically significant (P>0.05). Taken together, the *in vitro* and *in vivo* functional studies suggest that SMIs such as CAL-101 (i.e. competitive ATP binding inhibitors [34,36]) may be ineffective against the PI3Kδ-S isoform in AA PCa.

Cell-free PI3Kδ isoform kinase assay. The result of the exclusion of exon 20 (168 bp) in the *PIK3CD-S* variant is an in-frame deletion of 56 amino acids (residues 810-865) in the catalytic domain of the PI3Kδ-S isoform (**Fig. 7a**). To gain further insight into the functional differences between PI3Kδ isoforms, the interaction of PI3Kδ-L and -S with regulatory subunit p85α was investigated. Whole cell lysates from PC-3 cells overexpressing either His-tagged PI3Kδ-S or PI3Kδ-L were subjected to western analysis, demonstrating that each cell line expressed equivalent levels of their respective PI3Kδ isoform as well as equal p85α expression (**Fig. 7b**; left panel). Interestingly, co-IP of the PI3Kδ/p85α complex from whole cell lysates using an anti-His antibody demonstrated that p85α bound with 3-4-fold greater proficiency to PI3Kδ-L compared to p85α binding to PI3Kδ-S (**Fig. 7b**; right panel, column E).

Binding proficiency was inversely correlated with PI3Kδ isoform kinase activity (**Fig. 7c**; right panel).

Next, His-tagged PI3Kδ isoforms were purified from the lysates of PC-3 cells overexpressing either PI3Kδ-S or PI3Kδ-L using Ni-NTA resin columns. As shown in **Fig. 7d** (left and middle panels), purification of the PI3Kδ-S and -L isoforms was verified by western blotting using anti-His or anti-PI3Kδ antibodies. In addition, the Ni-NTA resin column purification approach resulted in the isolation of PI3Kδ isoforms that were no longer bound to p85α (**Fig. 7d**; far right panel, column E). The purified PI3Kδ isoforms (minus p85α) were incubated with vehicle, non-selective PI3K inhibitor wortmannin (100 nM) [37] or PI3Kδ-specific inhibitor CAL-101 (100 nM), and subjected to a PI3K activity assay. In the absence of bound p85α, kinase activity of PI3Kδ-L was equivalent to PI3Kδ-S (**Fig. 7e**, compare vehicle treatments). In agreement, siRNA-mediated knockdown of p85α in wild-type EA PCa cell lines VCaP and PC-3 was associated with an increase in invasive activity (**Supplementary Fig. S8**). Remarkably, wortmannin and CAL-101 significantly inhibited the activity of the PI3Kδ-L isoform, but not the PI3Kδ-S isoform (**Fig. 7e**). These results demonstrate that PI3Kδ-S maintains kinase activity even in the presence of SMIs, supporting the *in-vitro* and *in-vivo* results shown in **Figs. 5** and **6**.

Discussion

Emerging evidence indicates that, in addition to socioeconomic factors [3,38], biologic/genetic factors likely contribute to PCa health disparities among racial groups [39-51]. Immunohistochemical evaluation has revealed that epidermal growth factor receptor (EFGR) overexpression in PCa is more common in AA (~50% of patients) compared to EA patients (<20%) [52]. Moreover, a recent study in our

laboratory demonstrated that EGFR signaling is exacerbated by the presence of AA-specific miRNA-mRNA interactions, which appears to promote PCa aggressiveness in AA patients [20]. In addition to overexpression of EGFR, androgen receptor (*AR*) mRNA levels are 81% higher in AA PCa compared to EA PCa [53]. Interestingly, a polymorphic CAG repeat in exon 1 of the *AR* gene is frequently observed to be shorter in AA PCa compared to corresponding EA specimens [54,55]. The shorter repeats are associated with higher levels of *AR* gene transcription [56,57] and poorer prognostic indices, such as higher cancer grade and stage, along with increased incidents of metastasis and mortality [58]. Lastly, several gene profiling studies have identified cytokine, immune response, inflammatory, chemotaxis and pro-metastasis signaling pathways that are significantly enriched with differentially expressed genes in AA PCa compared to EA PCa [59-61].

In addition to DNA mutation and gene expression changes, alternative and/or aberrant RNA splicing has been demonstrated to augment oncogenic activity (e.g. cell proliferation, invasion, motility and therapeutic resistance) [10,15]. Alternative splicing of the gene encoding the Bcl-x apoptotic regulator results in anti-apoptotic Bcl-x_L and pro-apoptotic Bcl-x_S isoforms [62]. PCa xenografts expressing Bcl-x_L have been shown to exhibit castration-resistant tumor growth, and high levels of Bcl-x_L are associated with metastatic, castration-resistant human tumor samples [63]. Manipulation of splicing to decrease Bcl-x_L and increase Bcl-x_S levels has been shown to reduce tumor load in a murine melanoma tumor model [64]. Aberrant splicing of the androgen receptor pre-mRNA generates variants (e.g. *AR-V7*) lacking the C-terminal ligand binding domain [65]. AR-V7 has been associated with castrate resistant PCa, poorer clinical outcomes and resistance to androgen ablation/androgen receptor inhibition therapies [66-68].

The phenomenon of DS, much less global DS events, has not been adequately explored as a possible mechanism underlying PCa health disparities among racial groups. Potential involvement of the constitutively active *AR-V7* splice variant in PCa health disparities has been suggested in a recent study. Selective down-regulation of miR-212 observed in AA PCa compared to EA PCa is correlated with up-regulation of splicing factor hnRNP-H1 protein levels (miR-212 is predicted to target *hnRNP-H1* mRNA), up-regulation of the *AR-V7* variant, and resistance to anti-androgen therapy in PCa cell lines [69]. In contrast to this localized splicing event, our study reveals that DS on a global scale may be a critical molecular mechanism underlying PCa health disparities. In a comparison of AA PCa vs. EA PCa, DS events were found to be highly prevalent in cancer-associated genes and pathways (**Supplementary Table S1** and **S2**). Interestingly, the number of genes harboring DS events (2,520 genes) was ~3 times greater than the number of differentially expressed, but not differentially spliced, genes (886 genes). These findings have two major implications. First, alternative and/or aberrant splicing of pre-mRNAs may have a greater role than differential gene expression in driving PCa health disparities. Second, DS events identified in our study were statistically over-represented in oncogenic signaling pathways. In many cases, these same pathways are known to harbor a preponderance of gene mutations across different cancer types [22-24]. Thus, future studies are warranted to investigate the oncogenic consequences of interactions between gene mutations and DS events within the same pathway. Taken together, DS adds another layer of complexity to the existing molecular repertoire (e.g. differential gene mutation, expression, methylation; see review [45]) driving AA PCa aggressiveness.

Studies on alternative splicing indicate that approximately half of such events occurring in the coding sequence are in-frame, while the remaining events are frame-

shifts leading to truncated or extended C-terminal proteins [55,56]. Remarkably, 70% of AA-enriched/-specific variants in our composite oncogenic signaling pathway (**Fig. 2**) were in-frame, including *PIK3CD-S*, *FGFR2-S, FGFR3-S*, *TSC2-S*, *RASGRP2-b*, *ATM-S* and *GSK3-S* (see **Supplementary Table S5**). In stark contrast, only 27.3 % of EA-enriched/-specific DS events in our composite oncogenic signal pathway exhibited in-frame preservation (**Supplementary Table S5**), while the remaining 72.7% of EA-enriched DS variants, including *ITGA4-S*, *MET-S*, *NF1-S*, *RASGRP2-a*, *mTOR-S* and *BAK1-S*, were frame-shifted. Why the vast majority of DS events appear to be in-frame in AA PCa vs. frame-shifted in EA PCa remains unresolved (**Supplementary Table S3**). Presumably, the preponderance of AA in-frame events detected in oncogenic signaling pathways may be contributing to the more aggressive nature of AA PCa. Possible mechanisms that could drive differences in alternative splicing events include differential expression of *trans*-acting splicing factors [69] and/or single nucleotide polymorphisms in *cis*-acting splicing elements of alternatively spliced genes [70]. In fact, a number of splicing factor mRNAs appear to be overexpressed (e.g. *SRSF2*, *SRSF7*) in AA PCa compared to EA PCa [20,21]. Regarding the in-frame variants (i.e. *PIK3CD-L*, *FGFR3-L* and *TSC2-L*) detected in EA PCa and tested experimentally *in vitro* and/or *in vivo*, it is noteworthy that each conferred a less aggressive oncogenic phenotype compared to the corresponding in-frame variants detected in AA PCa (i.e. *PIK3CD-S*, *FGFR3-S* and *TSC2-S*).

Approximately one-third of the AA-enriched/-specific variants identified in AA PCa were likewise present in patient-matched NP specimens, whereas the remaining AA-enriched/-specific variants found in PCa were absent in patient-matched NP specimens and thus appear to be *de novo* events (i.e. occurring as NP evolved into PCa). Accordingly, the AA-enriched/-specific variants already present in

NP specimens have the potential to serve as inherent 'at-risk alleles' for poor PCa prognosis in the AA population. By comparison, the *de novo* appearance of tumor-specific variants may drive poorer outcomes. The *PIK3CD-S* variant would be an example of a potential AA 'at-risk allele' contributing to increased PCa aggressiveness upon disease presentation. Indeed, ectopic overexpression of the AA-enriched *PIK3CD-S* variant in PCa cell lines was demonstrated to enhance oncogenic potential (i.e. increased invasion, proliferation and AKT/mTOR signaling) compared to the corresponding EA-enriched variant *PIK3CD-L*. Moreover, genetic manipulation of AA cell line MDA PCa 2b PCa to favor expression of the *-S* variant over the *-L* variant likewise increased oncogenic behavior. Conversely, genetic manipulation in the opposite direction had the effect of decreasing oncogenic behavior in the AA PCa cell line. Interestingly, survival plots generated from TCGA RNA-Seq data demonstrate that a high S/L ratio is associated with significantly worse survival for PCa and trending for worse survival in both breast and colon cancer (**Supplementary Fig. S9**). Survival plots were not stratified by race as this information is not currently available in TCGA. Given the number patients analyzed, it seems highly probable that high S/L ratio values (besides being prevalent in AA patients) may also be associated with a subset of EA patients, suggesting that *PIK3CD-S* may be useful in predicting survival in all patients irrespective of race. Besides *PIK3CD-S*, we have identified an additional 732 potential 'at-risk alleles' (e.g. *ITGA4-L* and *MET-L*) that may be associated with poor PCa prognosis in the AA population. Further experimentation is needed to investigate whether these variants can serve as novel precision biomarkers to address PCa health disparities among racial groups. In contrast to the 'at-risk alleles', AA-enriched variants *FGFR-S* and *TSC2-S* were detected in AA PCa, but not in patient-matched NP specimens. The

appearance of these *de novo* variants during PCa formation may contribute to driving the more aggressive PCa phenotype observed in the AA population, since *in vitro* genetic manipulation favoring expression of these -*S* variants over the -*L* variants promoted oncogenesis in AA cell line MDA PCa 2b. It is noteworthy that three PCa-associated splice variants identified in previous studies, *Bcl-xL*, *FGFR2-IIIc* and *TMPRSS2-ERG* variants containing exon 8 [10,11,15], did not exhibit DS in our AA PCa vs. EA PCa comparison (see **Supplementary Table S1)**, suggesting that these variants may contribute to PCa progression and/or aggressiveness in a race-independent manner.

The identification of *PIK3CD-S*, a variant newly discovered and cloned in our study, as an 'at-risk allele' for PCa aggressiveness is germane given that PI3K signaling is aberrantly activated in a variety of cancers and PI3K inhibitors have been developed as targeted therapeutics [71,72]. Class IA PI3Ks consist of three isoforms, including PI3Kα, PI3Kβ and PI3Kδ. Unlike PI3Kα and PI3Kβ that are ubiquitously expressed, PI3Kδ appears to be preferentially expressed in leukocytes [73,74]. Previous studies have revealed a crucial role of PI3Kδ in development and progression of lymphoid and myeloid malignancies [34,75]. Interestingly, accumulating evidence suggests a functional role of PI3Kδ in promoting non-hematologic tumors as well. For example, overexpression of *PIK3CD* mRNA and/or PI3Kδ protein has been detected in glioblastoma [27], neuroblastoma [25], breast cancer [28] and PCa [26], and overexpression of *PIK3CD* mRNA has been implicated in promoting cell growth and survival in breast cancer and neuroblastoma [25,28]. Consistent with the aforementioned findings, our IHC experiments using a pan-PI3Kδ antibody likewise revealed strong expression of PI3Kδ protein in PCa specimens as well as PCa, breast cancer and colon cancer cell lines (**Supplementary Fig. S10**). Importantly, our study provides greater

granularity by being the first to demonstrate the relationship between expression of a race-enriched *PIK3CD* splice variant and cancer aggressiveness as well as resistance to small molecule inhibitors targeting PI3Kδ.

Aberrant pre-mRNA splicing has recently been demonstrated to mediate therapeutic resistance in multiple cancer types. For example, the constitutively active *AR-V7* splice variant (lacking exonic sequences encoding the ligand binding domain) confers resistance to enzalutamide and abiraterone acetate in castration-resistant PCa patients [76]. In addition, melanoma patients harboring *BRAF* splice variants encoding protein isoforms that are missing the RAS-binding domain exhibited resistance to the RAF inhibitor vemurafenib [77-79]. Noteworthy, these studies did not investigate whether variant expression and therapeutic responsiveness could be stratified along racial lines. We now provide evidence that the AA-enriched variant *PIK3CD-S*, cloned in this study for the first time, imparts PCa cell lines with significant resistance to small molecule inhibitors targeting PI3Kδ, as demonstrated in both *in vitro* assays and preclinical mouse models of PCa. This short variant is missing exon 20, encoding a 56 amino acid segment that is present in *PIK3CD-L*. Amino acids residing in the exon 20-encoded cassette, appear to be critical for the docking of CAL-101 and wortmannin. Indeed, molecular modeling studies predict that Glu826 and Val828 (missing in PI3Kδ-S isoform) undergo hydrogen bonding with CAL-101 [80]. Noteworthy, overall response of indolent lymphoma and chronic lymphocytic leukemia to CAL-101 ranges from 48% to 81% [81-83]. Given our findings, it would be of interest to determine if patients with primary resistance harbor malignant cells expressing the CAL-101-resistant *PIK3CD-S* variant, while responsive patients harbor malignant cells expressing the CAL-101-sensitive *PIK3CD-L* variant.

P85 regulatory subunits are known binding partners of class I PI3Ks, resulting in protein stabilization and inactivation of basal kinase activity [84,85]. Somatic mutations in *PIK3R1* (encoding p85α) have been identified that abrogate the inhibitory action of p85α on PI3Kα in cancers [86-89]. Our cell-free assays demonstrated that p85α binds more efficiently with PI3Kδ-L compared to PI3Kδ-S. This interaction appears to be responsible for the lower kinase activity exhibited by the long isoform, as disruption of binding led to a long isoform with increased kinase activity comparable to the short isoform (see **Fig. 7c** and **e**). The amino acid Asn334 located on the N-terminal side of PI3Kδ has been postulated to serve as a critical contact point with p85α [90]. Our findings suggest that amino acids 810-865, encoded by exon 20 and missing in PI3Kδ-S, may also contain essential amino acids required for efficient coupling to p85α. Alternatively, the presence of amino acids 810-865 permits PI3Kδ-L to adopt a conformation where Asn334 (and other amino acids) is available to interact with p85α.

The identification and functional validation of global alternative and aberrant mRNA splicing in cancer pathogenesis remains challenging and thus, largely unexplored. Here, we have undertaken such an analysis in the context of race-related aggressive PCa and have identified a large number of DS events in cancer-associated pathways in EA and AA PCa, with a subset of these events also being detected in patient-matched NP specimens. These events will have both biological and clinical consequences, case in point *PIK3CD-S*. The identification of novel splice variants as biomarkers and/or development of therapeutics targeting protein isoforms have the potential to reduce cancer health disparities.

Methods

Materials. EA PCa cell lines LNCaP (CRL-1740), VCaP (CRL-2876) and PC-3 (CRL-1435), and AA PCa cell line MDA PCa 2b (CRL-2422) were obtained from the American Type Tissue Collection (Manassas, VA). Primer sequences for RT-PCR are provided in **Supplementary Table S6**. SiRNAs were purchased from GE Dharmacon (Lafayette, CO) and sequences are as follows: Nonsense, CCA AAU UAU ACC UAC AUU GCU; siP_{20}, CCA ACA UCC AAC UCA ACA A; siP_j, UGA GGG AGG CCC UGG AUC GA; siF, CUC GAC UAC UAC AAG AAG A; siTSC2-ex20, CUG CGC UAU AAA GUG CUC A; siRASGRP2-ex11, CCA CAU CUC ACA GGA AGA A. siPIK3R1 Smart Pool (AGU AAA GCA UUG UGU CAU A, CCA ACA ACG GUA UGA AUA A, GAC GAG AGA CCA AUA CUU G, UAU UGA AGC UGU AGG GAA A).

Collection of PCa clinical specimens. Prostate biopsy samples were collected at the George Washington University Medical Faculty Associates according to an IRB-approved protocol (IRB#020867). High-quality PCa and patient-matched normal prostate (NP) biopsy cores from each of 20 AA and 15 EA primary PCa patients were collected and processed for the exon array analysis. PCa cores were determined by a pathologist to have Gleason scores of 6-7 (17 AA and 13 EA) or 8-9 (3 AA and 2 EA), while NP cores were diagnosed negative for cancer. There were no significant differences (t-test, $P>0.05$) between the two racial groups with respect to age (average age for AAs was 62.3 ± 8.2, average age for EAs was 63.3 ± 9.2) and Gleason score (range 6-8; Fisher's exact test, $P>0.05$). No distant metastasis was detected in the enrolled patients.

Exon array and statistical analyses. Total RNA was purified from PCa and patient-matched NP biopsy cores using the RNeasy micro kit (Qiagen, Valencia, CA). High quality RNA isolation was confirmed by using the Agilent Bioanalyzer as per manufacturer's protocol (Agilent Technologies, Santa Clara, CA). For exon array analysis, 1 μg of purified RNA sample from each biopsy core was interrogated with the Affymetrix Human Exon 1.0 ST GeneChip (Santa Clara, CA). Exon microarray data can be assessed at GEO using accession number GSE64331. The exon array raw data were subjected to quantile normalization, GC-content adjustment, RMA background correction and $\log_2$-transformation. Data analysis, data visualization and statistical analysis were performed using Partek Genomics Suite 6.6 software (Partek Incorporated, St. Louis, MO), as previously described [20,21]. Detection of differential expression at the gene level (gene-wise analysis) was performed in Partek using a One-Step Tukey's Biweight algorithm for detection of outlier probe-sets. Statistical analysis of exon expression data was based on ANOVA with multiple-correction testing using 10% False Discovery Rate (FDR) criterion [91]. DS events were modeled using the Alternative Splice ANOVA algorithm implemented in Partek together with selection of probe-sets exhibiting significant alternative splicing score determined at a 2% FDR [19]. Principal component analysis (PCA) plots and two-dimensional (2D) hierarchical clustering of exon level data were performed using Partek. DS events were tested for statistical over-representation in canonical signaling pathways by Fisher's exact test using the Ingenuity Pathway Analysis (IPA) program (Ingenuity Systems, Redwood City, CA).

RT-PCR validation of alternative splice variants in AA and EA PCa. Quantitative real time polymerase chain reaction (QRT-PCR) was performed using the 7300 Real-

Time PCR System (Applied Biosystems, Foster City, CA) to validate and quantify alternative splicing events. Primers were designed to amplify the flanking regions of skipped exons or the junctions across catenated exons of variant mRNAs (see illustration in **Fig. 3b**). Amplified RT-PCR products were quantified and normalized to house-keeping genes, *EIF1AX* and *PPA1*, as previously described [20,21]. Primer sequences for RT-PCR validation are listed in **Supplementary Table S1**.

Molecular cloning of *PIK3CD-S* and *PIK3CD-L* variants and overexpression of variants in PCa cell lines. RT-PCR was performed to amplify *PIK3CD-L* and *PIK3CD-S* transcript variants from purified RNA of PC-3, VCaP and MDA PCa 2b cells (ATCC, Manassas, VA). PC-3 and VCaP cells were maintained DMEM medium (Life Technologies, Gaithersburg, MD) supplemented with 10% fetal bovine serum (FBS), while MDA PCa 2b cells were grown in BRFF-HPC-1 medium (AthenES, Baltimore, MD) supplemented with 20% FBS. All the cell lines were grown at 37°C and 5% CO_2. Primers were designed according to NCBI reference sequences of *PIK3CD* mRNA (NM_005026.3). The forward primer contained the start codon (bold) (5'-**ATG**CCCCCTGGGGTGGACT-3') and the reverse primer was upstream of the stop codon (5'-CTGCCTGTTGTCTTTGGACA-3'). Full length PCR products were ligated into pcDNA3.1/V5-His TOPO vector (K4800-01, Invitrogen, Grand Island, NY) using the manufacturer's protocol. 8-10 independent clones were selected for each of the amplified *PIK3CD-L* and *PIK3CD-S* variants and sequence verified. The consensus sequences of *PIK3CD-S* and *PIK3CD-L* mRNAs were deposited to GeneBank (Accession number KU612116 and KU612117). The plasmids pcDNA3.1-PIK3CD-L/V5-His and pcDNA3.1-PIK3CD-S/V5-His were individually transfected

into the PCa cell lines (VCaP and PC-3) using the cationic lipid mediated method [20] to establish stable cell lines overexpressing *PIK3CD-L* or *PIK3CD-S.*

Functional analysis of PCa cell lines following transfection of siRNAs targeting the *PIK3CD-S* or the *PIK3CD-L* variant. VCaP and MDA PCa 2b cells were grown in DMEM medium with 10% FBS for 24h, then were transfected for 24h with siRNAs (50nM) designed to target splice variants of *PIK3CD*, *FGFR3*, *TSC2* or *RASGRP2* using DharmaFECT4 transfection reagent (Dharmacon, Lafayette, CO), according to the manufacturer's protocol. *In-vitro* functional assays, including cell proliferation and invasion were performed following siRNA transfections for 24 h. Cell proliferation and invasion assays were performed using BrdU Cell Proliferation Assay kit (Calbiochem, Billerica, MA) and the Matrigel Invasion Chambers (BD Biosciences, San Jose, CA), respectively, as previously described [20,21].

Antibodies. Antibodies used in western blot analysis were rabbit monoclonal antibodies for $pAKT^{Tyr308}$, $pAKT^{Ser473}$, AKT, pmTOR, mTOR, pS6 and S6 (#2965, #4058, #4691, #2971, #2983, #4857 and #2983, Cell Signaling Technology, Danvers, MA), rabbit polyclonal antibodies for His-tag (ab18184, Abcam, Cambridge, MA), PI3Kδ and β-actin (sc-55589 and sc-4778, Santa Cruz Biotechnology, Santa Cruz, CA). Horseradish peroxidase (HRP)-conjugated secondary antibodies for rabbit and mouse IgG were purchased from Southern Biotech (Birmingham, AL).

***In vivo* xenograft and metastasis models.** All animal work was approved by the George Washington University Institutional Animal Care and Use Committee (protocol A272). Four to six week old, male NOD-SCID mice were purchased from

the Jackson Laboratory (Bar Harbor, ME). To establish a PCa xenograft model, 2 × 10^6 PC-3 cells stably overexpressing *PIK3CD-L* or *PIK3CD-S* were subcutaneously injected into the left flank of NOD-SCID mice. Tumor xenograft growth was measured with calipers and the volume was determined as 1/2 × length × width^2. Mice were randomized into groups once the average tumor size reached ~200 mm^3 and treated with vehicle (PBS) or CAL-101 (50mg/kg) through daily i.p. injections. After 30 days, mice were sacrificed and the dissected xenografts were photographed and weighed.

To establish the PCa metastasis model, 1×10^6 PC-3 cells stably overexpressing *PIK3CD-L* or *PIK3CD-S* were injected into the tail vein of NOD-SCID mice. The mice were then treated with vehicle or CAL-101 (50mg/kg) via i.p. injections, 3 times a week. After 8 weeks, lungs of mice were harvested and stained with India ink and bleached with Fekete's solution (70% ethanol, 3.7% formaldehyde, 0.75 M glacial acetic acid). India ink-stained lungs were photographed and lung metastases were quantified using the NIH ImageJ program [92].

Purification of His-tagged PI3Kδ protein. PC-3 cells stably overexpressing *PIK3CD-L* or *PIK3CD-S* were maintained in DMEM media (Life Technologies, Gaithersburg, MD) supplemented with 10% fetal bovine serum (FBS). After growing the cells for 24 h, cell extracts were prepared and His-tagged PI3Kδ protein was purified using a column HisPur Ni-NTA purification kit (Pierce Biotechnology, Rockford, IL). Briefly, cell lysates were mixed with Ni-NTA resin and incubated at room temperature for 30 min. After incubation, the resin was washed with wash buffer (25mM imidazole, pH 7.4) and applied to a HisPur Ni-NTA spin column, centrifuged and wash buffer eluate discarded after centrifugations. His-tagged

proteins were eluted from the resin by adding one-resin-bed volume of elution buffer (250mM imidazole, pH 7.4). The purified PI3Kδ-His protein was mixed with 2× Laemmli sample buffer, boiled and analyzed by immunoblotting.

Co-immunoprecipitation (Co-IP) of PI3Kδ/p85 complex. Plasmids pcDNA3.1-PIK3CD-S/V5-His (or pcDNA3.1-PIK3CD-L/V5-His) and pSV-p85α (Addgene, Cambridge, MA) were co-transfected into PC-3 cells. After growing the cells for 48 h, the co-transfected cells were harvested and cells were lysed with RIPA lysis buffer (Santa Cruz Biotechnology, Santa Cruz, CA). The cell lysates were then subjected to Co-IP assays with anti-His antibody (ab18184, Abcam, Cambridge, MA) and immobilized on protein G-Sepharose beads (Thermo Scientific, Waltham, MA). Cell lysates and precipitates were subjected to western blotting, and visualized by enhanced chemiluminescence (ECL) system (Thermo Scientific, Waltham, MA).

***In vitro* assay of PI3Kδ activity.** PI3Kδ activity was evaluated with a PI3K activity/inhibitor assay kit (Millipore, Billerica, MA) according to the manufacturer's instructions. Briefly, purified His-tagged PI3Kδ-L or PI3Kδ-S isoform was pretreated with the PI3Kδ inhibitor (100nM of wortmannin or 100nM of CAL-101) or vehicle in 96 well plates for 10 min and subjected to a competitive ELISA. PIP2 substrate and kinase reaction buffer were added to the pretreated His-tagged PI3Kδ-L or PI3Kδ-S isoform and incubated at room temperature for 1 h. After incubation, biotinylated PIP3 and GST-GRP1 working solutions were added to the wells and the reaction samples were further incubated at room temperature for 1 h. Plates were washed three times with 1×TBST (50 mM Tris-Cl, pH 7.5. 150 mM NaCl) and incubated with SA-HRP (Streptavidin-Horseradish Peroxidase conjugate, 1.25 mg/ml) at room

temperature for 1 h. After incubation, plates were washed three times and incubated with 100 µl of TMB (3,3',5,5'-tetramethylbenzidine, 1 mg/ml) substrate solution at room temperature for 5-20 min. Reactions were stopped by adding 100 µl of stop solution and plates read at 450nm. The colorimetric signal was inversely proportional to the amount of PIP3 produced by PI3K activity and the relative amount of PIP3 produced was determined with a standard curve.

Additional methods can be accessed in the Supplementary Methods section.

References

1 Jemal, A. *et al.* Cancer statistics, 2007. *CA Cancer J Clin* **57**, 43-66 (2007).

2 Reddy, S., Shapiro, M., Morton, R., Jr. & Brawley, O. W. Prostate cancer in black and white Americans. *Cancer Metastasis Rev* **22**, 83-86 (2003).

3 Powell, I. J. Epidemiology and pathophysiology of prostate cancer in African-American men. *J Urol* **177**, 444-449 (2007).

4 Robbins, A. S., Whittemore, A. S. & Thom, D. H. Differences in socioeconomic status and survival among white and black men with prostate cancer. *Am J Epidemiol* **151**, 409-416 (2000).

5 Evans, S., Metcalfe, C., Ibrahim, F., Persad, R. & Ben-Shlomo, Y. Investigating Black-White differences in prostate cancer prognosis: A systematic review and meta-analysis. *Int J Cancer* **123**, 430-435 (2008).

6 Pan, Q., Shai, O., Lee, L. J., Frey, B. J. & Blencowe, B. J. Deep surveying of alternative splicing complexity in the human transcriptome by high-throughput sequencing. *Nat Genet* **40**, 1413-1415 (2008).

7 David, C. J. & Manley, J. L. Alternative pre-mRNA splicing regulation in cancer: pathways and programs unhinged. *Genes Dev* **24**, 2343-2364 (2010).

8 Chen, J. & Weiss, W. A. Alternative splicing in cancer: implications for biology and therapy. *Oncogene* **34**, 1-14 (2015).

9 Rajan, P., Elliott, D. J., Robson, C. N. & Leung, H. Y. Alternative splicing and biological heterogeneity in prostate cancer. *Nat Rev Urol* **6**, 454-460 (2009).

10 Mercatante, D. R., Mohler, J. L. & Kole, R. Cellular response to an antisense-mediated shift of Bcl-x pre-mRNA splicing and antineoplastic agents. *J Biol Chem* **277**, 49374-49382 (2002).

11 Oltean, S. *et al.* Alternative inclusion of fibroblast growth factor receptor 2 exon IIIc in Dunning prostate tumors reveals unexpected epithelial mesenchymal plasticity. *Proceedings of the National Academy of Sciences of the United States of America* **103**, 14116-14121, doi:10.1073/pnas.0603090103 (2006).

12 Hu, Y. *et al.* Delineation of TMPRSS2-ERG splice variants in prostate cancer. *Clin Cancer Res* **14**, 4719-4725, doi:10.1158/1078-0432.CCR-08-0531 (2008).

13 Attard, G. *et al.* Duplication of the fusion of TMPRSS2 to ERG sequences identifies fatal human prostate cancer. *Oncogene* **27**, 253-263, doi:10.1038/sj.onc.1210640 (2008).

14 Demichelis, F. *et al.* TMPRSS2:ERG gene fusion associated with lethal prostate cancer in a watchful waiting cohort. *Oncogene* **26**, 4596-4599, doi:10.1038/sj.onc.1210237 (2007).

15 Wang, J. *et al.* Pleiotropic biological activities of alternatively spliced TMPRSS2/ERG fusion gene transcripts. *Cancer Res* **68**, 8516-8524 (2008).

16 Heinlein, C. A. & Chang, C. Androgen receptor in prostate cancer. *Endocr Rev* **25**, 276-308 (2004).

17 Hu, R. *et al.* Ligand-independent androgen receptor variants derived from splicing of cryptic exons signify hormone-refractory prostate cancer. *Cancer Res* **69**, 16-22 (2009).

18 Sowalsky, A. G. *et al.* Whole transcriptome sequencing reveals extensive unspliced mRNA in metastatic castration-resistant prostate cancer. *Mol Cancer Res* **13**, 98-106, doi:10.1158/1541-7786.MCR-14-0273 (2015).
19 Fan, W., Stirewalt, D. L., Radich, J. P. & Zhao, L. Comparison of Two Methods for Detecting Alternative Splice Variants Using GeneChip((R)) Exon Arrays. *Int J Biomed Sci* **7**, 172-180 (2011).
20 Wang, B. D. *et al.* Identification and Functional Validation of Reciprocal microRNA-mRNA Pairings in African American Prostate Cancer Disparities. *Clinical cancer research : an official journal of the American Association for Cancer Research* **21**, 4970-4984 (2015).
21 Wang, B. D. *et al.* Androgen receptor-target genes in african american prostate cancer disparities. *Prostate cancer* **2013**, 763569 (2013).
22 Network, T. C. G. A. R. Comprehensive genomic characterization defines human glioblastoma genes and core pathways. *Nature* **455**, 1061-1068 (2008).
23 Ding, L. *et al.* Somatic mutations affect key pathways in lung adenocarcinoma. *Nature* **455**, 1069-1075 (2008).
24 Network, T. C. G. A. R. Integrated genomic analyses of ovarian carcinoma. *Nature* **474**, 609-615 (2012).
25 Boller, D. *et al.* Targeting the phosphoinositide 3-kinase isoform p110delta impairs growth and survival in neuroblastoma cells. *Clinical cancer research : an official journal of the American Association for Cancer Research* **14**, 1172-1181 (2008).
26 Jiang, X., Chen, S., Asara, J. M. & Balk, S. P. Phosphoinositide 3-kinase pathway activation in phosphate and tensin homolog (PTEN)-deficient prostate cancer cells is independent of receptor tyrosine kinases and mediated by the p110beta and p110delta catalytic subunits. *J Biol Chem* **285**, 14980-14989 (2010).
27 Knobbe, C. B. & Reifenberger, G. Genetic alterations and aberrant expression of genes related to the phosphatidyl-inositol-3'-kinase/protein kinase B (Akt) signal transduction pathway in glioblastomas. *Brain Pathol* **13**, 507-518 (2003).
28 Tzenaki, N. *et al.* High levels of p110delta PI3K expression in solid tumor cells suppress PTEN activity, generating cellular sensitivity to p110delta inhibitors through PTEN activation. *Faseb J* **26**, 2498-2508 (2012).
29 Glickman, M., Malek, R. L., Kwitek-Black, A. E., Jacob, H. J. & Lee, N. H. Molecular cloning, tissue-specific expression, and chromosomal localization of a novel nerve growth factor-regulated G-protein- coupled receptor, nrg-1. *Mol Cell Neurosci* **14**, 141-152 (1999).
30 Korenchuk, S. *et al.* VCaP, a cell-based model system of human prostate cancer. *In Vivo* **15**, 163-168 (2001).
31 Navone, N. M. *et al.* Establishment of two human prostate cancer cell lines derived from a single bone metastasis. *Clinical cancer research : an official journal of the American Association for Cancer Research* **3**, 2493-2500 (1997).
32 Herman, S. E. *et al.* Phosphatidylinositol 3-kinase-delta inhibitor CAL-101 shows promising preclinical activity in chronic lymphocytic leukemia by antagonizing intrinsic and extrinsic cellular survival signals. *Blood* **116**, 2078-2088 (2010).

33 Lannutti, B. J. *et al.* CAL-101, a p110delta selective phosphatidylinositol-3-kinase inhibitor for the treatment of B-cell malignancies, inhibits PI3K signaling and cellular viability. *Blood* **117**, 591-594 (2011).
34 Fruman, D. A. & Rommel, C. PI3Kdelta inhibitors in cancer: rationale and serendipity merge in the clinic. *Cancer Discov* **1**, 562-572 (2011).
35 Yang, J. *et al.* Pathological axonal death through a MAPK cascade that triggers a local energy deficit. *Cell* **160**, 161-176, doi:10.1016/j.cell.2014.11.053 (2015).
36 Berndt, A. *et al.* The p110 delta structure: mechanisms for selectivity and potency of new PI(3)K inhibitors. *Nat Chem Biol* **6**, 117-124, doi:10.1038/nchembio.293 (2010).
37 Arcaro, A. & Wymann, M. P. Wortmannin is a potent phosphatidylinositol 3-kinase inhibitor: the role of phosphatidylinositol 3,4,5-trisphosphate in neutrophil responses. *Biochem J* **296 (Pt 2)**, 297-301 (1993).
38 Jones, B. A. *et al.* Explaining the race difference in prostate cancer stage at diagnosis. *Cancer Epidemiol Biomarkers Prev* **17**, 2825-2834 (2008).
39 Haiman, C. A. *et al.* Multiple regions within 8q24 independently affect risk for prostate cancer. *Nat Genet* **39**, 638-644 (2007).
40 Robbins, C. *et al.* Confirmation study of prostate cancer risk variants at 8q24 in African Americans identifies a novel risk locus. *Genome Res* **17**, 1717-1722 (2007).
41 Powell, I. J. *et al.* CYP3A4 genetic variant and disease-free survival among white and black men after radical prostatectomy. *J Urol* **172**, 1848-1852 (2004).
42 Bangsi, D. *et al.* Impact of a genetic variant in CYP3A4 on risk and clinical presentation of prostate cancer among white and African-American men. *Urol Oncol* **24**, 21-27 (2006).
43 Kittles, R. A. *et al.* A common nonsense mutation in EphB2 is associated with prostate cancer risk in African American men with a positive family history. *J Med Genet* **43**, 507-511 (2006).
44 Robbins, C. M., Hooker, S., Kittles, R. A. & Carpten, J. D. EphB2 SNPs and sporadic prostate cancer risk in African American men. *PloS one* **6**, e19494 (2011).
45 Powell, I. J. & Bollig-Fischer, A. Minireview: the molecular and genomic basis for prostate cancer health disparities. *Molecular endocrinology* **27**, 879-891, doi:10.1210/me.2013-1039 (2013).
46 Rose, A. E. *et al.* Copy number and gene expression differences between African American and Caucasian American prostate cancer. *Journal of translational medicine* **8**, 70, doi:10.1186/1479-5876-8-70 (2010).
47 Nock, N. L. *et al.* Polymorphisms in glutathione S-transferase genes increase risk of prostate cancer biochemical recurrence differentially by ethnicity and disease severity. *Cancer causes & control : CCC* **20**, 1915-1926, doi:10.1007/s10552-009-9385-0 (2009).
48 Tang, D. *et al.* Elevated polycyclic aromatic hydrocarbon-DNA adducts in benign prostate and risk of prostate cancer in African Americans. *Carcinogenesis* **34**, 113-120, doi:10.1093/carcin/bgs326 (2013).
49 Devaney, J. M. *et al.* Genome-wide differentially methylated genes in prostate cancer tissues from African-American and Caucasian men. *Epigenetics* **10**, 319-328, doi:10.1080/15592294.2015.1022019 (2015).

50 Kittles, R. A. *et al.* A common nonsense mutation in EphB2 is associated with prostate cancer risk in African American men with a positive family history. *Journal of medical genetics* **43**, 507-511, doi:10.1136/jmg.2005.035790 (2006).
51 Petrovics, G. *et al.* A novel genomic alteration of LSAMP associates with aggressive prostate cancer in African American men. *EBioMedicine* **2**, 1957-1964, doi:10.1016/j.ebiom.2015.10.028 (2015).
52 Shuch, B. *et al.* Racial disparity of epidermal growth factor receptor expression in prostate cancer. *J Clin Oncol* **22**, 4725-4729 (2004).
53 Gaston, K. E., Kim, D., Singh, S., Ford, O. H., 3rd & Mohler, J. L. Racial differences in androgen receptor protein expression in men with clinically localized prostate cancer. *J Urol* **170**, 990-993 (2003).
54 Sartor, O., Zheng, Q. & Eastham, J. A. Androgen receptor gene CAG repeat length varies in a race-specific fashion in men without prostate cancer. *Urology* **53**, 378-380 (1999).
55 Irvine, R. A., Yu, M. C., Ross, R. K. & Coetzee, G. A. The CAG and GGC microsatellites of the androgen receptor gene are in linkage disequilibrium in men with prostate cancer. *Cancer Res* **55**, 1937-1940 (1995).
56 Chamberlain, N. L., Driver, E. D. & Miesfeld, R. L. The length and location of CAG trinucleotide repeats in the androgen receptor N-terminal domain affect transactivation function. *Nucleic Acids Res* **22**, 3181-3186 (1994).
57 Kazemi-Esfarjani, P., Trifiro, M. A. & Pinsky, L. Evidence for a repressive function of the long polyglutamine tract in the human androgen receptor: possible pathogenetic relevance for the (CAG)n-expanded neuronopathies. *Human molecular genetics* **4**, 523-527 (1995).
58 Giovannucci, E. *et al.* The CAG repeat within the androgen receptor gene and its relationship to prostate cancer. *Proc Natl Acad Sci U S A* **94**, 3320-3323 (1997).
59 Reams, R. R. *et al.* Microarray comparison of prostate tumor gene expression in African-American and Caucasian American males: a pilot project study. *Infectious agents and cancer* **4 Suppl 1**, S3 (2009).
60 Wallace, T. A. *et al.* Tumor immunobiological differences in prostate cancer between African-American and European-American men. *Cancer Res* **68**, 927-936 (2008).
61 Powell, I. J. *et al.* Genes associated with prostate cancer are differentially expressed in African American and European American men. *Cancer Epidemiol Biomarkers Prev* **22**, 891-897 (2013).
62 Akgul, C., Moulding, D. A. & Edwards, S. W. Alternative splicing of Bcl-2-related genes: functional consequences and potential therapeutic applications. *Cellular and molecular life sciences : CMLS* **61**, 2189-2199, doi:10.1007/s00018-004-4001-7 (2004).
63 Sun, A. *et al.* Androgen receptor-dependent regulation of Bcl-xL expression: Implication in prostate cancer progression. *The Prostate* **68**, 453-461, doi:10.1002/pros.20723 (2008).
64 Bauman, J. A., Li, S. D., Yang, A., Huang, L. & Kole, R. Anti-tumor activity of splice-switching oligonucleotides. *Nucleic acids research* **38**, 8348-8356, doi:10.1093/nar/gkq731 (2010).

65 Hu, R. *et al.* Ligand-independent androgen receptor variants derived from splicing of cryptic exons signify hormone-refractory prostate cancer. *Cancer research* **69**, 16-22, doi:10.1158/0008-5472.CAN-08-2764 (2009).
66 Hornberg, E. *et al.* Expression of androgen receptor splice variants in prostate cancer bone metastases is associated with castration-resistance and short survival. *PloS one* **6**, e19059, doi:10.1371/journal.pone.0019059 (2011).
67 Dehm, S. M., Schmidt, L. J., Heemers, H. V., Vessella, R. L. & Tindall, D. J. Splicing of a novel androgen receptor exon generates a constitutively active androgen receptor that mediates prostate cancer therapy resistance. *Cancer research* **68**, 5469-5477, doi:10.1158/0008-5472.CAN-08-0594 (2008).
68 Antonarakis, E. S. *et al.* AR-V7 and resistance to enzalutamide and abiraterone in prostate cancer. *The New England journal of medicine* **371**, 1028-1038, doi:10.1056/NEJMoa1315815 (2014).
69 Yang, Y. *et al.* Dysregulation of microRNA-212 Promotes Castration Resistance via hnRNPH1-Mediated Regulation of AR and AR-V7: Implications for Racial Disparity of Prostate Cancer. *Clinical cancer research : an official journal of the American Association for Cancer Research* (2015).
70 Blencowe, B. J. Alternative splicing: new insights from global analyses. *Cell* **126**, 37-47, doi:10.1016/j.cell.2006.06.023 (2006).
71 Courtney, K. D., Corcoran, R. B. & Engelman, J. A. The PI3K pathway as drug target in human cancer. *J Clin Oncol* **28**, 1075-1083 (2010).
72 Ciraolo, E., Morello, F. & Hirsch, E. Present and future of PI3K pathway inhibition in cancer: perspectives and limitations. *Curr Med Chem* **18**, 2674-2685 (2011).
73 Clayton, E. *et al.* A crucial role for the p110delta subunit of phosphatidylinositol 3-kinase in B cell development and activation. *J Exp Med* **196**, 753-763 (2002).
74 Jou, S. T. *et al.* Essential, nonredundant role for the phosphoinositide 3-kinase p110delta in signaling by the B-cell receptor complex. *Molecular and cellular biology* **22**, 8580-8591 (2002).
75 Castillo, J. J., Furman, M. & Winer, E. S. CAL-101: a phosphatidylinositol-3-kinase p110-delta inhibitor for the treatment of lymphoid malignancies. *Expert Opin Investig Drugs* **21**, 15-22 (2012).
76 Nakazawa, M., Antonarakis, E. S. & Luo, J. Androgen receptor splice variants in the era of enzalutamide and abiraterone. *Horm Cancer* **5**, 265-273 (2014).
77 Shi, H. *et al.* Acquired resistance and clonal evolution in melanoma during BRAF inhibitor therapy. *Cancer Discov* **4**, 80-93 (2014).
78 Wellbrock, C., Karasarides, M. & Marais, R. The RAF proteins take centre stage. *Nat Rev Mol Cell Biol* **5**, 875-885 (2004).
79 Freeman, A. K., Ritt, D. A. & Morrison, D. K. The importance of Raf dimerization in cell signaling. *Small GTPases* **4**, 180-185 (2013).
80 Berndt, A. *et al.* The p110delta structure: mechanisms for selectivity and potency of new PI(3)K inhibitors. *Nat Chem Biol* **6**, 117-124 (2010).
81 Gopal, A. K. *et al.* PI3Kdelta inhibition by idelalisib in patients with relapsed indolent lymphoma. *N Engl J Med* **370**, 1008-1018 (2014).

82 Brown, J. R. *et al.* Idelalisib, an inhibitor of phosphatidylinositol 3-kinase p110delta, for relapsed/refractory chronic lymphocytic leukemia. *Blood* **123**, 3390-3397 (2014).
83 Shah, A. & Mangaonkar, A. Idelalisib: A Novel PI3Kdelta Inhibitor for Chronic Lymphocytic Leukemia. *Ann Pharmacother* **49**, 1162-1170 (2015).
84 Vanhaesebroeck, B., Guillermet-Guibert, J., Graupera, M. & Bilanges, B. The emerging mechanisms of isoform-specific PI3K signalling. *Nat Rev Mol Cell Biol* **11**, 329-341, doi:10.1038/nrm2882 (2010).
85 Yu, J. *et al.* Regulation of the p85/p110 phosphatidylinositol 3'-kinase: stabilization and inhibition of the p110alpha catalytic subunit by the p85 regulatory subunit. *Molecular and cellular biology* **18**, 1379-1387 (1998).
86 Jaiswal, B. S. *et al.* Somatic mutations in p85alpha promote tumorigenesis through class IA PI3K activation. *Cancer Cell* **16**, 463-474, doi:10.1016/j.ccr.2009.10.016 (2009).
87 Shekar, S. C. *et al.* Mechanism of constitutive phosphoinositide 3-kinase activation by oncogenic mutants of the p85 regulatory subunit. *J Biol Chem* **280**, 27850-27855, doi:10.1074/jbc.M506005200 (2005).
88 Philp, A. J. *et al.* The phosphatidylinositol 3'-kinase p85alpha gene is an oncogene in human ovarian and colon tumors. *Cancer Res* **61**, 7426-7429 (2001).
89 Chan, T. O. *et al.* Small GTPases and tyrosine kinases coregulate a molecular switch in the phosphoinositide 3-kinase regulatory subunit. *Cancer Cell* **1**, 181-191 (2002).
90 Amzel, L. M. *et al.* Structural comparisons of class I phosphoinositide 3-kinases. *Nat Rev Cancer* **8**, 665-669, doi:10.1038/nrc2443 (2008).
91 Benjamini, Y. & Hochberg, Y. Controlling the false discovery rate: a practical and powerful approach to multiple testing. *J R Statist Soc* **57**, 289-300 (1995).
92 Fukuda, H. *et al.* Host-derived MMP-13 exhibits a protective role in lung metastasis of melanoma cells by local endostatin production. *Br J Cancer* **105**, 1615-1624, doi:10.1038/bjc.2011.431 (2011).

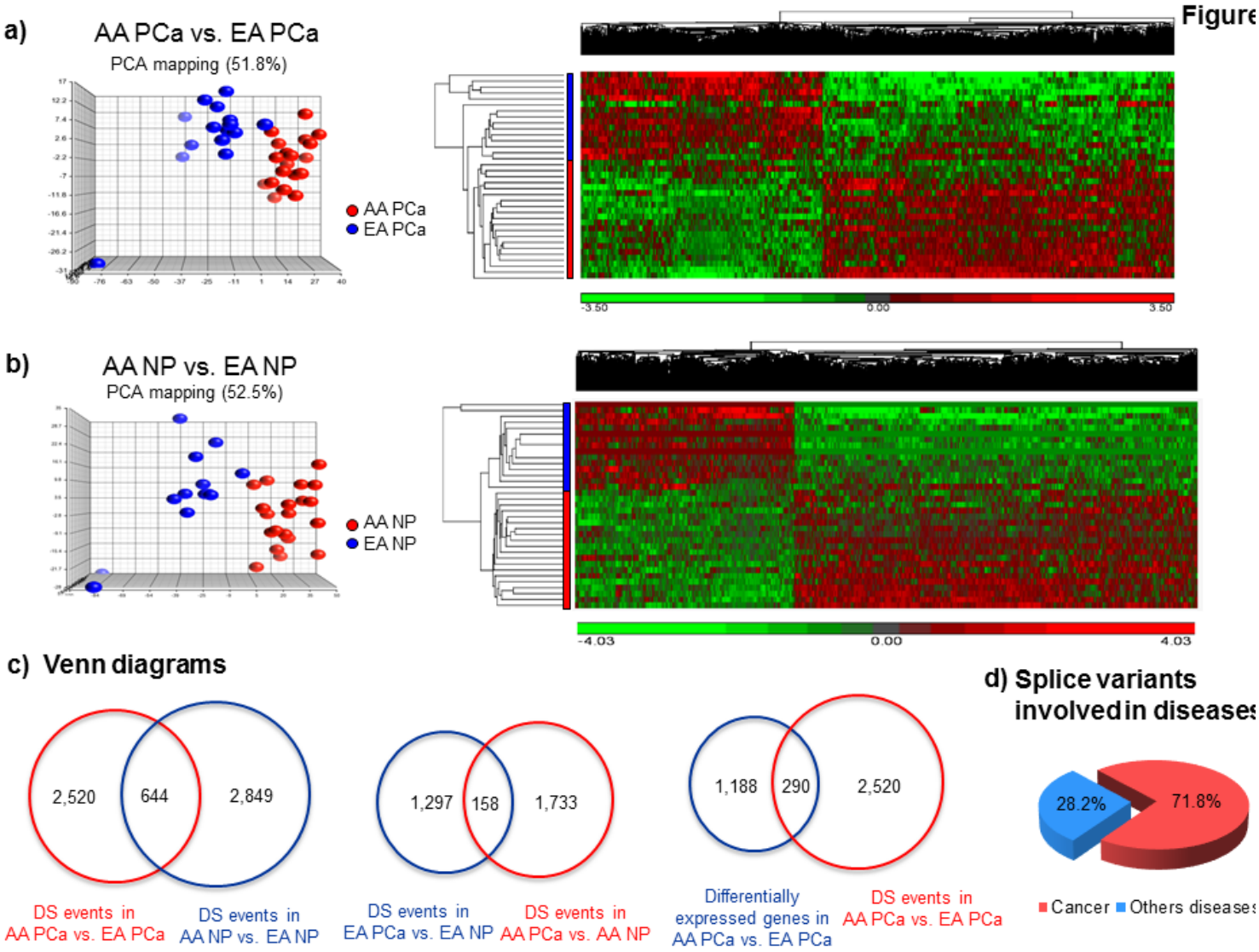

Fig. 1. Heatmaps of alternative splicing differences in AA PCa vs. EA PCa and AA NP vs. EA NP specimens. (a) PCA plot and 2D-clustergram depicting 3,112 significant differentially expressed exons in 20 independent AA PCa vs. 15 independent EA PCa specimens. (b) PCA plot and 2D-clustergram depicting 3,384 significant differentially expressed exons in 20 AA NP vs. 15 EA NP specimens. AA and EA specimens are represented by red and blue circles/bars, respectively. Rows represent specimens and columns represent exons in hierarchical clustergrams. Log2 expression values of exons were subjected to 2D unsupervised hierarchical clustering using average linkage method and Euclidean distance. (c) Venn diagrams of DS events in AA PCa vs. EA PCa and AA NP vs. EA NP, DS events in EA PCa vs. EA NP and AA PCa vs. AA NP and differentially expressed genes in AA PCa vs. EA PCa and DS events in AA PCa vs. EA PCa. d) Majority of the genes with DS events in AA PCa vs. EA PCa were functionally associated with cancer. Top 3 ‘other diseases’ were gastrointestinal disease, organismal injury and abnormalities and reproductive system disease.

Figure 2

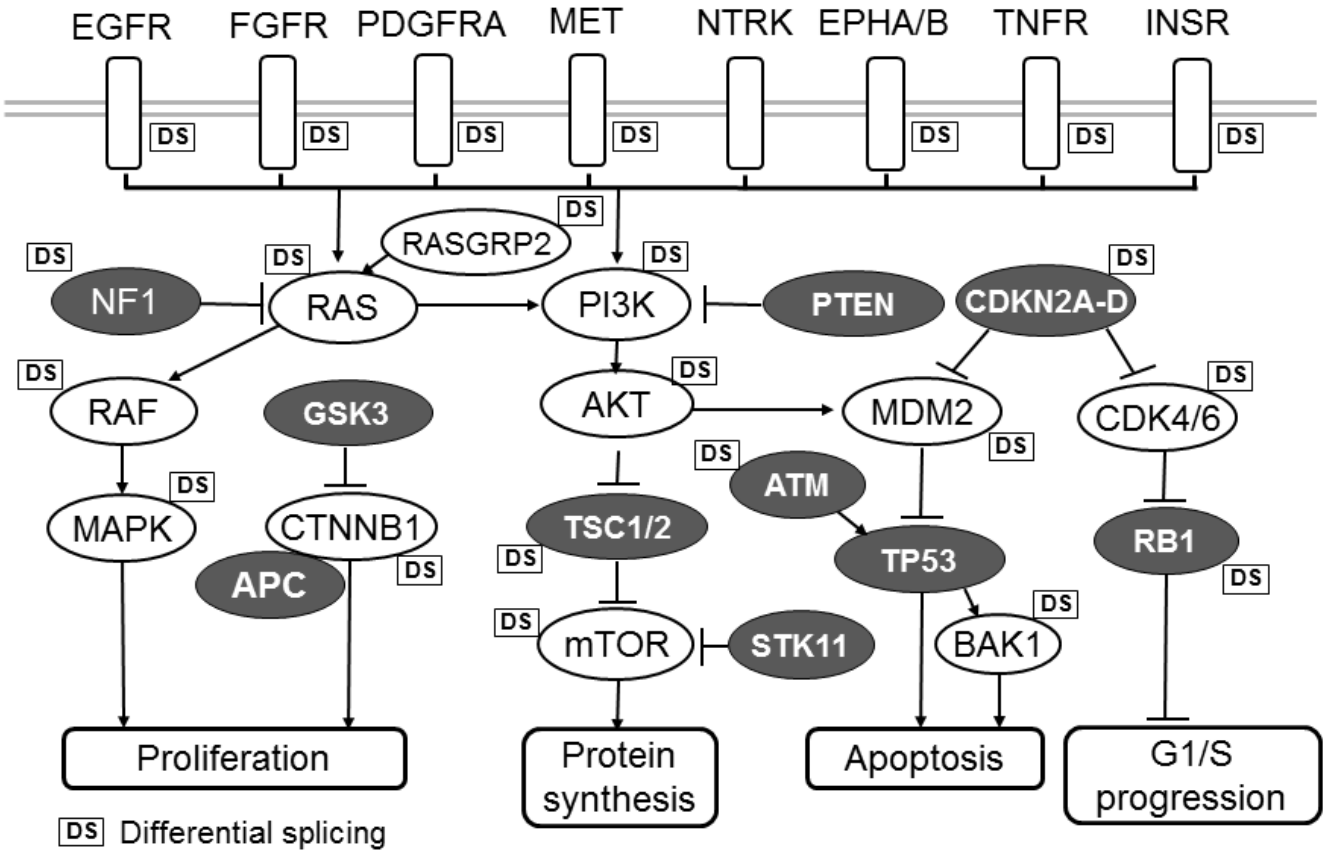

Fig. 2. Representation of differential splicing events in a composite oncogenic signaling pathway. DS events in AA PCa vs. EA PCa were frequently detected in multiple oncogenic signaling pathways. Depicted pathway is a composite of PI3K/AKT/mTOR, RAS/RAF/MAPK, CDK/RB1, MDM2/TP53 and WNT/GSK3/CTNNB1/APC signaling. Open figures indicate oncogenes and closed figures indicate tumor suppressor genes. “DS” indicates that a differential alternative splicing event was detected for a particular oncogene or tumor suppressor gene.

Figure 3

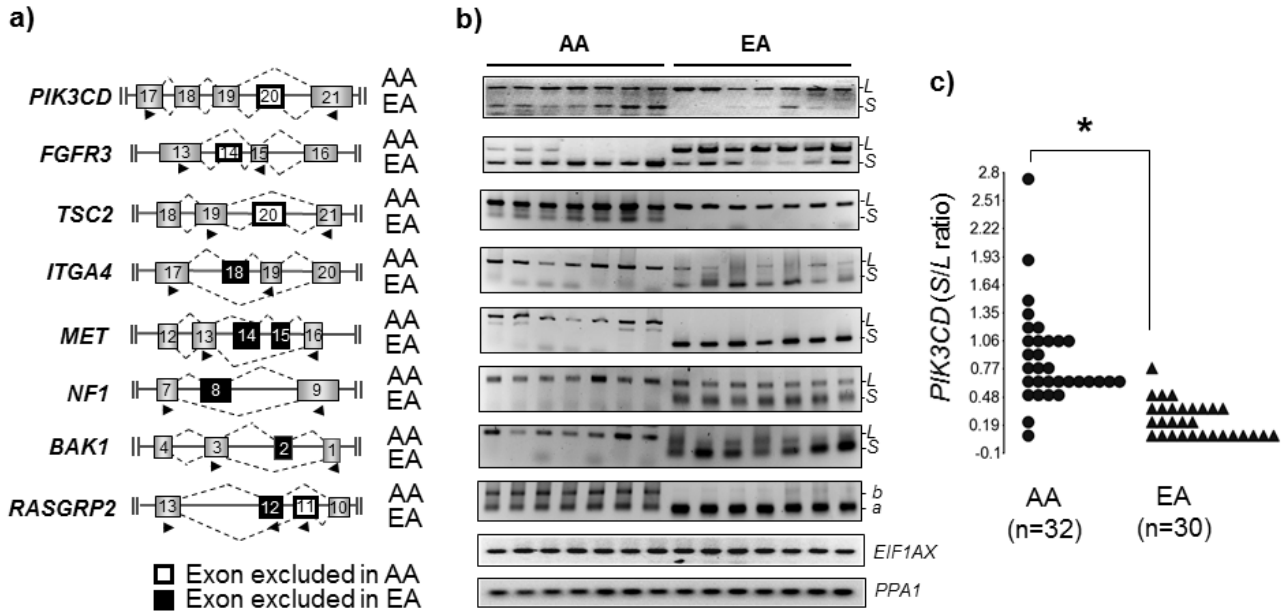

Fig. 3. Validation of differential alternative splicing of oncogenes and tumor suppressor genes in AA vs EA PCa specimens. (a) Schematic representation of DS events within the indicated genes in AA PCa (top dashed lines connecting exons) and EA PCa (bottom dashed lines) based on Alternative Splicing ANOVA model. Closed arrowheads below exons represent primer location in QRT-PCR validation of alternatively spliced transcripts. (b) Representative RT-PCR results validating race-specific/-enriched variant transcripts in either AA PCa or EA PCa specimens. Shown are the RT-PCR results for the AA-specific/-enriched variants *PI3KCD-S, FGFR3-S, TSC2-S, ITGA4-L, MET-L, NF1-L, BAK1-L* and *RASGRP2-b*; and EA-specific/-enriched variants *PIK3CD-L*, *FGFR3-L*, *TSC2-L, ITGA4-S, MET-S, NF1-S, BAK1-S* and *RASGRP2-a*. Each lane represents an RT-PCR result from an independent PCa specimen that was also interrogated in exon array experiments. RT-PCR of *EIF1AX* and *PPA1* transcripts served as loading controls. QRT-PCR results is summarized in **Supplementary Fig. S4**. (c) Additional validation and quantification of the ratio of the AA-enriched *PI3KCD-S* (short) variant and the race-independent *PI3KCD-L* (long) variant in a separate cohort of PCa patient specimens. RNA was isolated from n=32 AA PCa and n=30 EA PCa specimens and subjected to QRT-PCR. Shown is a plot of the ratio of S/L. *EIF1AX* and *PPA1* transcripts served as internal normalization controls. * $P < 0.05$ using Student t-test.

Figure 4

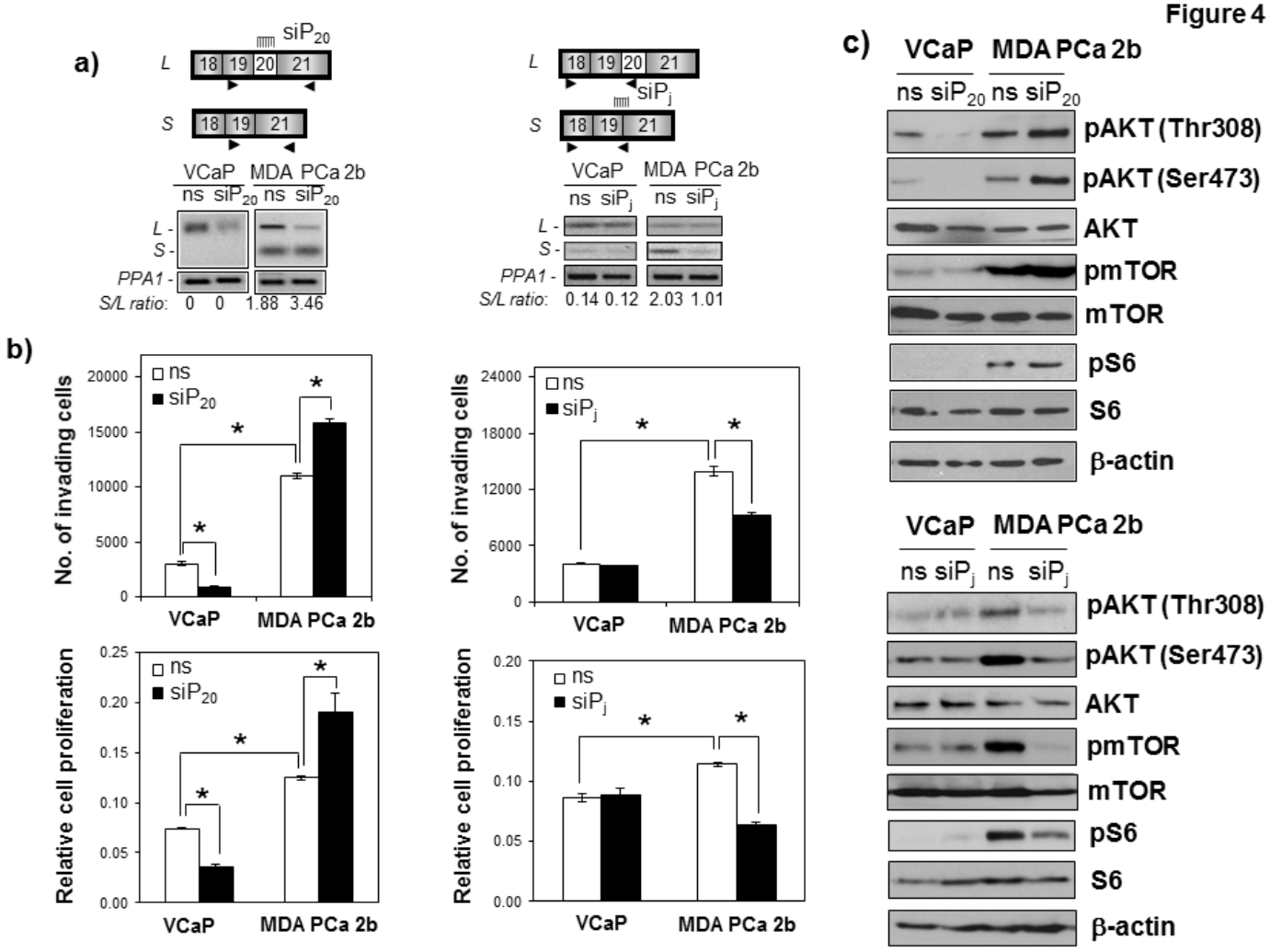

Fig. 4. Selective knockdown of the AA-enriched *PIK3CD-S* variant or race-independent *PIK3CD-L* variant has opposing effects on proliferation, invasion and AKT/mTOR signaling in AA PCa cells. (a) RT-PCR of *PIK3CD-L* and *PIK3CD-S* variants following knockdown in the EA PCa cell line VCaP and AA PCa cell line MDA PCa 2b. Specific knockdown of the *PIK3CD-L* variant (left panel) was accomplished with an exon 20-targeting siRNA (siP_{20}), while knockdown of the *PIK3CD-S* variant (right panel) was achieved with an siRNA targeting the region spanning exons 19 and 21 (siP_j). Closed arrowheads below exons represent primer location for QRT-PCR validation of alternatively spliced transcript knockdowns. Knockdown efficiency of siP_{20} and siP_j siRNAs was determined by the *S/L* ratio derived from RT-PCR reactions. ns = nonsense siRNA treatment. Representative images of n = 4 independent knockdown experiments. (b) Proliferation and invasion of VCaP and MDA PCa 2b following knockdown of the *PIK3CD-S* (left panel) or *PIK3CD-L* variant (right panel). Data presented as mean ± SEM of n=3-5 independent experiments for each treatment group. **P* < 0.05 by ANOVA with post-hoc Tukey. (c) Western blot analysis of AKT/mTOR signaling following knockdown of the *PIK3CD-L* (top panel) or *PIK3CD-S* variant (bottom panel) in VCaP and MDA PCa 2b. Level of AKT, mTOR and ribosomal S6 kinase activities is reflected by the amount of phospho-AKT (pAKT), phospho-mTOR (pmTOR) and phospho-ribosomal protein S6 (pS6) immunoblotting, respectively. β-actin served as loading control. Representative images from n = 3-4 independent western blot experiments.

Figure 5

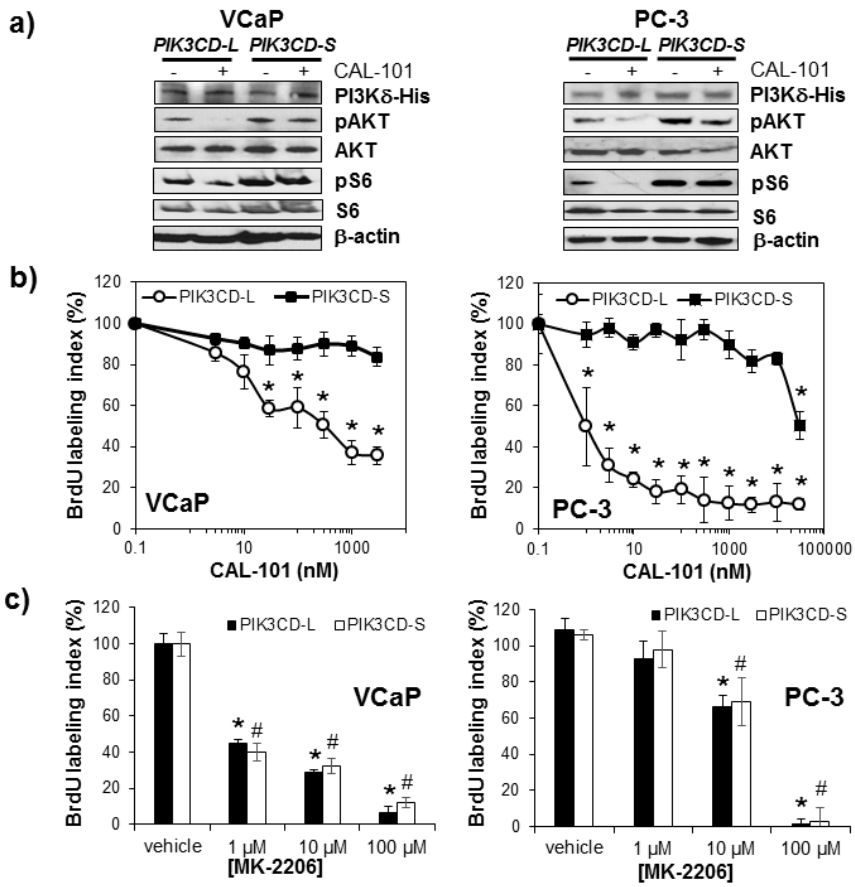

Fig. 5. PI3Kδ-S, but not PI3Kδ-L, is resistant to small molecule inhibition of PI3K/AKT/mTOR signaling and proliferation. (a) Assessment of PI3K/AKT/mTOR signaling following treatment with vehicle (saline) or CAL-101 (100 nM, 24 hrs). PI3K/AKT/mTOR signaling was assessed by western blot analysis with phospho-antibodies to AKT (pAKT) and S6 ribosomal protein (pS6). β-actin served as a loading control. His-tag antibody was used to demonstrate equal expression of His-tagged variant PI3Kδ protein in stably transfected cell lines. Representative images from n = 3-4 independent western blot experiments. *Significantly different from corresponding vehicle control, $P < 0.05$ by ANOVA with Dunnett's post-hoc test. (b) Proliferation in VCaP and PC-3 cells stably overexpressing the *PIK3CD-S* variant or *PIK3CD-L* variant following treatment with vehicle (saline) or selective PI3Kδ small molecule inhibitor CAL-101 (24 hrs), and (c) treatment with vehicle (saline) or selective AKT small molecule inhibitor MK-2206 (24 hrs). Proliferation was assessed using a BrdU labeling assay. Data presented as the mean ± SEM of n=4-6 independent experiments for each treatment group. * or #Significantly different from corresponding vehicle control, $P < 0.05$ by ANOVA with Dunnett's post-hoc test.

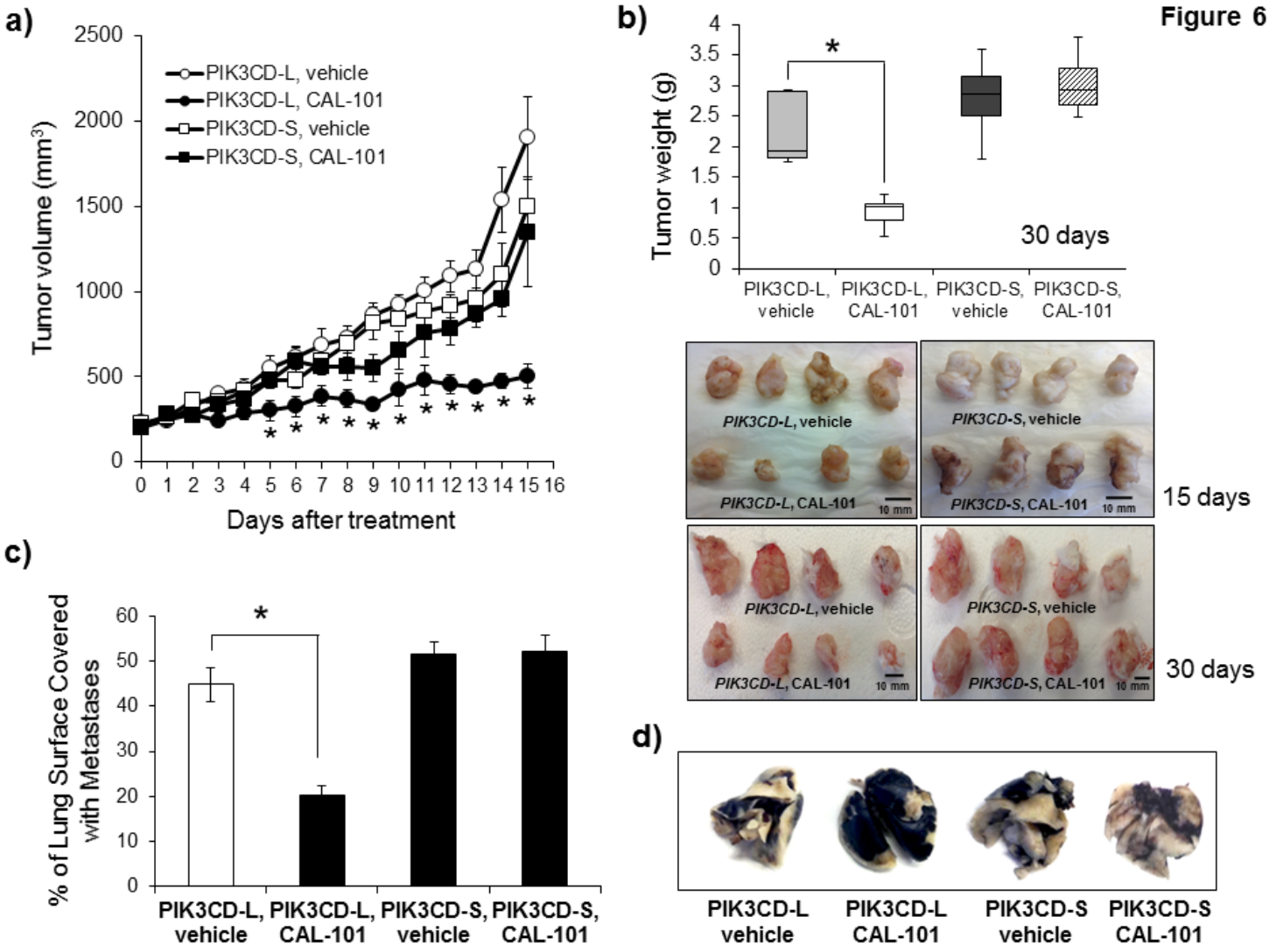

Figure 6

Fig. 6. PI3Kδ-S, but not PI3Kδ-L, is resistant to small molecule inhibition of xenograft growth and metastasis. (a) Growth of PC-3 cells stably overexpressing the *PIK3CD-S* variant in NOD-SCID mice is resistant to CAL-101 treatment (50mg/kg i.p. 3 times a week). In contrast, growth of PC-3 cells stably overexpressing the *PIK3CD-L* variant is sensitive to CAL-101 treatment. Data represent the mean tumor size ± SEM of n=10 independent mice for each treatment group at each time point. *Significantly different from saline treated group, $P < 0.05$ by ANOVA with post-hoc Tukey. (b) Tumor weights and gross morphology of tumor xenografts from (a). Box-and-whisker plot represents mean xenograft weight in mice after 30-day vehicle or CAL-101 treatment. *$P < 0.05$ by ANOVA with Dunnett's post-hoc test; n=10 independent mice for each treatment group. (c) Quantification of lung metastases in NOD-SCID mice. PC-3 cells stably overexpressing *PIK3CD-L* or *PIK3CD-S* were injected into the tail vein of NOD-SCID mice treated with vehicle or CAL-101 (50mg/kg i.p. 3 times a week). After 8 weeks, lungs were harvested and stained with India ink and bleached with Fekete's solution for visualization of metastatic nodules (white-colored areas). Data presented as mean ± SEM of n = 10 for each treatment group. *$P < 0.05$ by ANOVA with Dunnett's post-hoc test. (d) Representative India ink-stained lungs from treatment groups analyzed in (c).

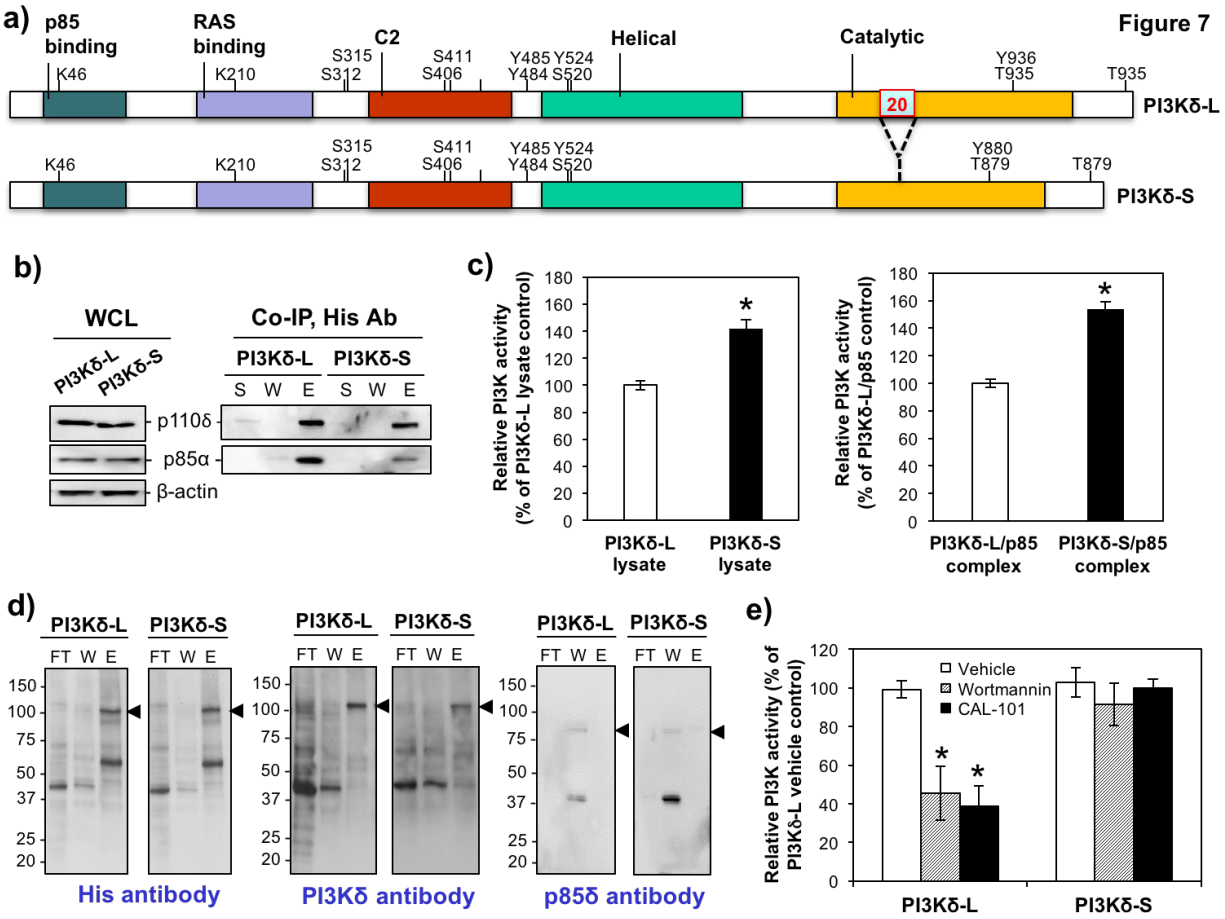

Fig. 7. Cell-free kinase assay of PI3Kδ isoforms and tertiary structure modeling of PIK3δ-small molecule inhibitor interactions. (a) Schematic representation of protein domains of PI3Kδ-L and -S isoforms. Adaptor (p85)-binding, RAS binding, C2, helix and catalytic domains are highlighted. Phosphorylation and ubiquitination sites (S, T, Y and K) and the region encoded by exon 20 (56 amino acids) residing in the catalytic domain are indicated. (b) Co-immunoprecipitation (Co-IP) of PI3Kδ/p85 complex followed by western blot, (c) and PI3K activity assays. S, supernatant; W, wash fraction; E, eluted fraction. Blots are representative of 3-5 independent experiments with similar results. Anti-His antibody was used in the Co-IP experiments and anti-His, anti-p85α and anti-actin antibodies were used in the western blotting. *Significantly different kinase activities in total lysates of PI3Kδ-S vs. PI3Kδ-L expressing cells, or purified PI3Kδ-S/p85 vs. PI3Kδ-L/p85 complexes. $P < 0.05$ using Student t-test. Data presented as mean ± SEM of n = 4 for each treatment group. (d) Purification of His-tagged PI3Kδ-L and -S isoforms. Western blot analysis of Ni-NTA resin-purified PI3Kδ isoforms from transfected PC-3 cells using His and PI3Kδ antibodies. FT, flow-through; W, wash fraction; E, eluted fraction. Blots are representative of 4 independent experiments with similar results. Closed arrowheads indicate PI3Kδ isoforms. (e) Cell-free kinase assay of L and S isoforms of PI3Kδ in the presence of vehicle (PBS), 100nM wortmannin or 100nM CAL-101. *Significantly different from vehicle control-treated PI3Kδ-L isoform. $P < 0.05$ by ANOVA with Dunnett's post-hoc test. Data presented as mean ± SEM of n = 4-5 for each treatment group.